

REFERENCE USE

SLAC-146
LBL-750
UC-34
(TH), (EXP),
(EXPI), (ACC)

PARTICLE PHYSICS WITH
POSITRON-ELECTRON-PROTON COLLIDING BEAMS

STANFORD LINEAR ACCELERATOR CENTER
STANFORD UNIVERSITY
Stanford, California 94305

and

LAWRENCE BERKELEY LABORATORY
UNIVERSITY OF CALIFORNIA
Berkeley, California 94720

PREPARED FOR THE U. S. ATOMIC ENERGY COMMISSION
UNDER CONTRACTS NO. AT(04-3)-515 and W-7045-eng-48

April 1972

Printed in the United States of America. Available from National Technical Information Service, U. S. Department of Commerce, 5285 Port Royal Road, Springfield, Virginia 22151.
Price: Printed Copy \$3.00; Microfiche \$0.95.

The following persons (in alphabetical order) contributed to this report.

SLAC

M. Allen
S. M. Berman
S. J. Brodsky
M. Davier
S. D. Drell
S. Flatté (U.C. Santa Cruz)
F. J. Gilman
M. Lee
P. Morton
A. Odian
J. Rees
B. Richter
M. Schwartz
S. Wojcicki

LBL

G. Abrams
G. Chew
C. Friedberg
A. Garren
G. Gidal
G. Goldhaber
J. Kadyk
S. Parker (University of Hawaii)
A. Sessler
L. Smith
M. L. Stevenson
M. Suzuki

PREFACE

In June of 1971 a group of physicists from the Frascati Laboratory, CERN, the Lawrence Berkeley Laboratory, and the Stanford Linear Accelerator Center began a study of the feasibility of achieving a large reaction rate in very high energy electron-proton collisions through the use of colliding beam techniques. The results of this work were presented in a paper at the 1971 Accelerator Conference in Geneva,¹ which described a positron-electron-proton colliding beam complex, and which excited a great deal of interest in the physics community.

In the fall of 1971 a joint LBL, SLAC study was organized whose first goal was a more thorough study of the physics potential of a high reaction rate electron-proton colliding beam facility (the physics interest in the electron-positron component of the complex had been extensively investigated previously²). The results of this study are presented in this report and indicate that this type of colliding beam complex will vastly expand our horizons in the study of the structure and interactions of the elementary particles.

With the very exciting positive conclusions of the joint study on the experimental potential of the complex, a new phase of the study has begun to work out a detailed conceptual design of the machines. This work is still in an early stage. In the system of rings under study, electrons and/or positrons are stored in one storage ring and protons in another. The two rings, which presumably will be of about the same size and will occupy the same housing, intersect each other in a number of interaction regions where the optical properties of the guide fields are specially tailored to produce strongly focused beams with small transverse beam dimensions and concomitant short local betatron-oscillation wave lengths (low- β) as well as low dispersion. These are the conditions for high luminosity and the luminosities for which the system is designed are around $10^{32} \text{ cm}^{-2} \text{ sec}^{-1}$. With electrons or positrons in the electron ring and protons in the proton ring, e^+p or e^-p collisions can be achieved; e^+e^- collisions are provided by storing both species in the electron

-
1. C. Pellegrini et al., Proc. of the International Accelerator Conference (1971).
 2. S. M. Berman, S. D. Drell, J. R. Rees, B. Richter, Report No. SLAC-TN-71-22 (August 1971).

ring. All particles in each ring will be concentrated into one or more short bunches which will encounter each other only in interaction regions.

Studies are underway of the required high voltage rf system, the phase-space densities which can be achieved for the protons, the design of interaction-region optical systems for both rings which permit flexibility of experimental arrangements, the beam instabilities to be expected and alternative methods of injection into both rings. This work is not covered in this report which concentrates on the physics interest and the experimental physics possibilities.

TABLE OF CONTENTS

	<u>Page</u>
I. Introduction	1
A. Deep Inelastic Lepton Scattering	2
B. Weak Interactions	3
C. Photoproduction	4
D. Electron-Positron Colliding Beams	5
II. Large Momentum Transfer Reactions (deep inelastic electron scattering and weak interactions)	6
A. Physics Considerations on Deep Inelastic Electron Scattering	6
B. Physics Considerations on Weak Interactions	8
C. Experimental Considerations	14
References	29
III. Photoproduction (Almost Real Photons)	30
A. Introduction	30
B. Physics of Photoproduction	31
IV. Physics with Electron-Positron Colliding Beam Rings	42
A. Behavior of the Total e^-e^+ Hadronic Cross Section as a Function of Energy	45
B. Inclusive Production Cross Sections with Detection of One Hadron	47
C. Inclusive Production Cross Sections with Detection of Several Hadrons	49
D. Heavy Leptons	49
E. Weak Intermediate Meson (W) Pairs	52
F. Two-Photon Processes	53
References	58

LIST OF FIGURES

	<u>Page</u>
Section II	
1. Total intermediate vector meson (W) production cross section in lepton-hadron collisions	11
2a. Final lepton kinematics for inelastic lepton scattering of 15 GeV leptons incident on 70 GeV protons	15
2b. Final lepton kinematics for inelastic lepton scattering of 15 GeV leptons incident on 70 GeV protons	17
3. Inelastic lepton scattering event rate using	
1) $\frac{d^2\sigma}{dx dy} = \frac{\pi\alpha^2}{s} \left(\frac{1-x}{x^2} \right) \left(\frac{1}{2} + \frac{1-y}{y^2} \right)$ (assuming $\nu W_2 \approx \frac{1}{2}(1-x)$ and $W_1/W_2 = \nu^2/Q^2$). 2) $0.01 \leq x$ and $y \leq 1$.	
3) 100% detection eff. 4) Luminosity = $10^{32} \text{ (cm}^2 \text{ sec)}^{-1}$. . .	19
4. Neutrino event rate for spin 1/2 parton model assuming	
1) $\sigma_{\nu n} = 0.8 \nu_{\text{max}} 10^{-38} \text{ cm}^2$. 2) $\nu (\beta \equiv \underline{W}_2) \propto (1-x)$.	
3) $\sigma_R = \sigma_S = 0$, i. e., spin 1/2 parton model.	
4) 100% detection eff. 5) Luminosity = $10^{32} \text{ (cm}^2 \text{ sec)}^{-1}$. . .	21
5. The kinematic y dependence of the factors in front of σ_L , σ_S and σ_R as defined in Eq. (8b)	22
6. How scaling for neutrino events would be broken by the existence of 53 GeV intermediate vector boson. Error bars correspond to a 10 day run. The variable $x = Q^2/2M\nu$; $y = \nu/\nu_{\text{max}}$	24
7. How scaling for electron events would be broken by the existence of a neutral intermediate boson of the Weinberg type for $\theta_W = 0$ and 90 degrees. Error bars are typical of those for a 10 day run at PEP with $\mathcal{L} = 10^{32} \text{ (cm}^2 \text{ sec)}^{-1}$. . .	26
Section III	
1. Graphs of the electron momentum transfer $ q^2 $ versus the lab scattering angle in mrad for various final electron energies	36

	<u>Page</u>
2. Variation of $d\sigma/dE$ as a function of the final electron energy E for incident energy $E_0 = 15$ GeV, minimum angle of detection $\theta_{\min} = 10$ mrad and maximum detection angle 35 mrad with $\sigma_T = 100 \mu\text{b}$	38
 Section IV	
1. Electron-positron annihilation into hadrons and muons via the one photon channel	43
2. Final states X produced by two photon annihilation in lepton-lepton collisions	44
3. Electron-positron annihilation into two back-to-back jets	50
4. The rising two photon annihilation cross sections as a function of total c.m. energy plotted along with the falling one photon annihilation channel	55

I. INTRODUCTION

The successful operation of high energy electron-positron and proton-proton colliding beam machines has led us to consider the possibility of both a large increase of energy in electron-positron interactions, and of applying the colliding beam technique to achieving an even larger increase of energy in electron-proton interactions. In this report we discuss the kinds of physics which can be studied with a positron-electron-proton colliding beam complex (PEP). We find that in electron-proton collisions, PEP is capable of an enormous extension of parameters in traditional electron machine experiments (inelastic electron scattering, photoproduction, etc.), and in addition will open the field of weak interactions to practical experimentation with a well understood, well controlled probe--the electron. In electron-positron collisions, PEP is capable of investigating particle production with a pure and beautifully simple photon probe at center-of-mass energies comparable to the highest-energy conventional accelerators now under construction.

In order to give the physics study a focus, we have chosen the energies of the beams in PEP to be about 15 GeV for electrons and positrons, and 72 GeV for protons. This gives a center-of-mass energy for electron-proton collisions of 65 GeV which is the same as that which would be available if a 2000-GeV beam from a conventional accelerator strikes a stationary hydrogen target (there is no economically feasible way of reaching these energies with a conventional accelerator). The energy of 65 GeV in the c.m. is also in the same range as the ISR proton-proton machine of 50-GeV c.m. energy and also corresponds to the region where the weak interactions are expected to become comparable to the electromagnetic interactions. The 30-GeV c.m. energy available in electron-positron collisions matches the c.m. energy available in proton-proton collisions from a 500-GeV NAL. It should be emphasized that the detailed accelerator studies which will define the final parameters of a PEP device are in an early phase and still higher energies are under consideration.

The physics possibilities with PEP can be divided into roughly four areas. These are:

1. Deep inelastic electron scattering where the reaction would be

$$e^-(e^+) + P \rightarrow e^-(e^+) + \text{anything}$$

with the study of both the scattered lepton as well as the nature of the hadronic states composing the "anything".

2. Weak interactions where the process would be

$$eP \rightarrow \nu + \text{anything}$$

especially in the region of large momentum transfer to the "anything".

3. Photoproduction where the scattered electron produces a spectrum of essentially real photons for the study of γP reactions.
4. Electron-positron colliding beams where the reaction is

$$e^-e^+ \rightarrow \text{hadrons, leptons, photons.}$$

We summarize below some of the essential physics of these four categories. The main body of this report will further discuss these four categories in more detail.

A. Deep Inelastic Lepton Scattering

Inelastic electron-proton scattering plays an essential and unique role in the investigation of the structure of the hadrons. The known electromagnetic field generated by the scattered electron interacts with the local electromagnetic current of the proton and thus can probe the structure of the nucleon at arbitrarily small distances. This local interaction is in sharp contrast to hadron-hadron scattering in which the basic interaction between the particles is more complex. By varying the energy and angle of the scattered electron it is possible to "tune" or vary the virtual photon's mass Q^2 over a large range. In particular it is possible to achieve virtual photon masses whose square is negative and whose magnitude is much greater than the proton mass and therefore allows for collisions in an asymptotic region not available in accelerators using a fixed mass projectile.

Experiments on inelastic scattering at SLAC, where both the mass and energy of the virtual photon are large, have yielded profound and unexpected results. These results show that the cross sections do not depend independently on both the mass and energy of the photon, but instead on their ratio. This "scaling" behavior has led to major new concepts in our understanding of hadronic structure in terms of a possible substructure within the hadron that is composed of point-like constituents (partons). The greatly enhanced center-of-mass energy of a PEP facility would extend the measurements of

deep inelastic scattering far into the unknown region. With the example parameters used here the virtual photon energy would reach to 2000 GeV and its mass to 65 GeV compared to an energy of 20 GeV and a mass of 5 GeV at the present SLAC frontier.

Confirmation of the scaling behavior at these larger values of energy and mass would give support to these new ideas while observation of violations of scaling would indicate a new energy scale for hadronic phenomena perhaps associated with the production of new particles and of a "size" for the constituents themselves. Other general and fundamental features to be studied for large photon masses include the applicability of Regge theory analyses, the validity of sum rules based on current algebra, and the "fragmentation" of very massive virtual photons into jets of secondary hadrons.

Thus, this unique feature of a PEP facility, the study of deep inelastic scattering, will yield results on one of the most significant problems in particle physics.

B. Weak Interactions

A PEP system opens very exciting new possibilities for studying weak interactions in an energy range when they begin to become "strong". Essentially the same theory as proposed by Fermi for β decays with energy releases of the order of kilovolts is used presently as the framework for interpreting neutrino-induced reactions with energies of 1 to 10 GeV. Since the effective Fermi interaction coupling constant is energy dependent, the range of validity of this theory already extends from couplings of order $GE^2 = 10^{-15}$ to $GE^2 = 10^{-4}$.

If the scaling phenomena observed in deep inelastic scattering is assumed to hold also for the weak interactions, as would be implied at least in part by the conserved vector current (CVC) idea, then with the Fermi theory one is led to the conjecture that the total weak interaction cross section will continue to grow quadratically with the center-of-mass energy. This has the startling consequence that at energies in the PEP region the weak interactions with their inherent violation of parity and strangeness would have grown in strength to be comparable to the electromagnetic interaction. In fact in the region of the largest momentum transfer accessible for the particular example of PEP

parameters used in this study, the scaling hypothesis indicates that the deep inelastic electromagnetic cross section is smaller than the weak process.

Experiments with PEP will show either that the weak interaction is no longer "weak" or that the Fermi theory in its simple form breaks down. The discovery of a failure in the Fermi theory would in itself be of the first magnitude in importance; additionally one could then entertain hopes of discovering the mechanism of breakdown. If a W boson, for example, were the source of a major failure of Fermi theory, its mass might be sufficiently low (≈ 25 GeV) that W particles could be produced by PEP.

C. Photoproduction

Here the proton beam interacts with a spectrum of photons having all energies up to a maximum energy equal to the incoming electron. For almost-real photons of low virtual masses the physics is roughly equivalent to that accessible to a real photon beam of maximum energy ~ 2000 GeV, incident on a stationary proton. If the photon is "tagged" by a coincidence measurement of the scattered electron, its energy and polarization as well as mass will be known. A variety of photon-nucleon experiments then becomes possible, including total cross sections, single-particle inclusive cross sections and certain reactions leading to special final states. The reactions with hadronic final states will bear similarities to the analogous states produced by a hadronic projectile. With the energies available at PEP, comparisons and correlations may be made on states complementary to those studied with both the ISR and NAL, thus enriching the general body of knowledge on hadronic reactions in the next decade of energies.

In addition the photon-proton reactions allow for the possibility of elastic and inelastic Compton scattering and their comparison with fundamental dispersion theory as well as with conjectures about the structures of the proton. Certain tests of quantum electrodynamics (QED) also are feasible, such as muon pair production. These tests would complement similar studies made with the e^-e^+ facility and could extend our comparison of experiments with QED theory to distances of order 10^{-16} cm or less.

D. Electron-Positron Colliding Beams

When the electron and positron collide, a state of hadrons or of a lepton pair with the unique quantum numbers of one unit of angular momentum and odd charge conjugation is produced by an electromagnetic current in the reaction

$$\begin{aligned} e^+ + e^- &\rightarrow \gamma^* \rightarrow \text{hadrons} \\ &\rightarrow e^+ e^- \\ &\rightarrow \mu^+ \mu^-. \end{aligned}$$

The virtual time-like photon γ^* has an invariant (mass)² equal to the square of the total of the collision energy $s=(2E)^2$. The production cross sections, energy dependences, correlations and multiplicities of final particles can all be studied in this one pure angular momentum channel produced by a single γ .

This is in contrast to electroproduction, photoproduction, or hadronic projectile production where all angular momenta are present and contribute to the reaction. Many direct tests of hadronic structures are thus permitted by the e^-e^+ colliding beam which are not possible in any other manner. In addition, recent analyses indicate that final states produced by two virtual photons can also be studied in detail.

Besides the possibility of studying the structure of hadrons created by the pure annihilation channel, the e^-e^+ facility has the additional unique feature of producing pairs of leptonic-like particles up to large masses (of order 1/2 the center-of-mass energy). Should these particles have only electromagnetic and weak interactions (such as the ω -meson) then the colliding electron-positron beam reaction will be the most direct and simple manner for their observation.

These examples show the wealth of physics possibilities that are accessible by the combining of PEP and e^-e^+ colliding beams. The information already acquired at lower energies surely indicates that experiments in the higher energy regime will have an extremely important impact on our understanding of the nature of elementary particles.

II. LARGE MOMENTUM TRANSFER REACTIONS (Deep Inelastic Electron Scattering and Weak Interactions)

A. Physics Considerations on Deep Inelastic Electron Scattering

Inelastic electron-proton scattering plays an essential and unique role in the investigation of the structure of the hadrons. The known electromagnetic field generated by the scattered electron interacts with the local electromagnetic current of the proton and thus can probe the structure of the nucleon at arbitrarily small distances. This is in sharp contrast to hadron-hadron scattering in which the basic interaction between the particles is both unknown and diffuse. By varying the scattered electron's energy and angle we are able to study virtual photon-proton collisions as a function of photon energy, mass, and polarization. This unique capability of "tuning" the photon mass $\sqrt{q^2}$ in lepton-induced reactions has opened up a significant new area of study of hadron structure.

The inclusive inelastic electron scattering experiment carried out at SLAC over the last few years have yielded profound and unexpected results. The experimental results have given evidence of a scale-invariant behavior of the proton and neutron structure functions which strongly hint at a rich substructure within the nucleon itself. Instead of being functions of the two independent variables, the energy transfer, $\nu = p \cdot q/M$, and the invariant momentum transfer squared q^2 , the measured nucleon structure functions are observed to behave as universal functions of the dimensionless variable $\omega = 2M\nu/|q^2|$, as first conjectured by Bjorken, and remain large in the presently accessible SLAC range ($2 \lesssim \nu \lesssim 20$ GeV, $1 \lesssim |q^2| \lesssim 25$ GeV²). The enormous center-of-mass energy of PEP will greatly extend these inclusive measurements far into the unknown region ($\nu \lesssim 2000$ GeV, and $|q^2| \lesssim 4000$ GeV) and will critically test theory. The observation of scale-invariant behavior in the PEP energy range would imply that we are observing asymptotic features of the proton structure, and would strongly support the main hypothesis of the parton and light-cone models: that the carriers of the electromagnetic current within the hadrons are structureless and light. Observation of scaling breakdown, on the other hand, would imply a new scale for hadronic phenomena, as would be required, e.g., if there are thresholds for parton or quark production. Scaling breakdown could also reflect form factor structure of the partons

themselves, nonscaling behavior of Regge and Pomeron contributions, a non-scaling variation of the longitudinal/transverse virtual photon cross section ratio R , or even a breakdown of quantum electrodynamics as in the Lee-Wick and Weinberg theories. Thus the experimental support or failure of scaling in the new energy regime represents one of the most significant problems in particle physics. Further checks of sum rules, duality constraints, and threshold properties, such as the Drell-Yan formula, are also important areas of study in the inclusive PEP measurements.

Further clues to the fundamental substructure of the nucleon must come from the detailed study of the properties of the final state in deep inelastic e - p scattering, and this will be a dominant focus at PEP. The analysis of the multiplicities, momentum distributions, and correlations of the final state will distinguish many theoretical models — whether, for example, the constituents of the proton have a clustered, rather than a homogeneous or gas-like, distribution. The semi-inclusive measurements, $e + p \rightarrow e' + X + (\text{anything})$ are important tests of various parton model scaling predictions and provide a critical check of dynamical symmetry for various particles X of a multiplet. Parton models also predict that at the large q^2 and ν available at PEP, final hadrons will emerge with a sharp jet-like distribution. Of course, an even more dramatic possibility would be the production of new constituent particles, but in any event, the analysis of the properties of the final state hadrons and the search for dominant channels is of critical theoretical interest.

Another very interesting area of possible PEP measurements concerns the photon mass dependence of specific electroproduction channels. For example, does the effective "size" of the electromagnetic interaction become smaller with increasing q^2 , as predicted in various models. There are also questions in the area of diffractive production and vector meson production — especially the role of vector dominance and s -channel helicity conservation — which will be important to investigate at the large ν , q^2 , and momentum transfers possible at PEP.

The above discussion is predicted on the dominance of the lowest order electromagnetic one-photon exchange contribution. Possible two-photon exchange contributions could be determined by comparing electron-proton with positron-proton scattering at PEP. In general, the analysis of radiative

corrections at PEP are not expected to be more difficult than the analysis performed for the present MIT-SLAC inelastic experiments.

There are, however, higher order electromagnetic processes which will be especially exciting to measure at PEP. For example, the measurements of the elastic and inelastic wide-angle bremsstrahlung processes $e+p \rightarrow e+\gamma+p'$, and $e+p \rightarrow e+\gamma+(\text{anything})$ can not only test the timelike and spacelike electron propagator in the standard Bethe-Heitler amplitude at masses up to 65 GeV, but also leads to a measurement of the virtual Compton amplitude $\gamma(q^2) + p \rightarrow \gamma + p'$, $\gamma(q^2) + p \rightarrow \gamma + (\text{anything})$. It is especially interesting to measure the difference of electron and positron bremsstrahlung (a natural possibility for PEP) since the difference of cross sections is proportional to the part of the Compton amplitude which interferes with the Bethe-Heitler contribution. This is a very important measurement related to the real part of the elastic Compton amplitude. The determination of the q^2 and energy dependence of this quantity (especially confirmation of energy-independent terms in the amplitude due to point-like substructure) will be critical in testing further predictions of the parton model and would represent a unique feature of experiments at PEP. Further, measurement of the order α^4 processes such as $ep \rightarrow e\mu^+\mu^- + (\text{anything})$, allows for the determination of the virtual Compton amplitude with one spacelike and one timelike photon.

These examples show the wealth of possible physics that can be studied in the deep inelastic region. The information already acquired at lower energies surely indicates that new information at PEP energies will have an extremely important impact on the understanding of nucleon structure.

B. Physics Considerations on Weak Interactions

Fermi envisioned his theory of weak interactions to apply to β -decay where the energies released were of order kilovolts. Essentially this same theory gives the framework for understanding neutrino induced reactions where the c.m. energies are of order 1 to 5 GeV. Since the basic weak interaction proposed by Fermi involves the weak coupling constant G with dimensions of inverse energy squared, we see that his idea of an elementary point interaction has been valid for a (dimensionless) coupling constant region spanning more than 11 orders of magnitude from $G E_\beta^2 = 10^{-15}$ ($E_\beta \approx 10$ keV) to $G E_\nu^2 = 2 \times 10^{-4}$ ($E_\nu \approx 5$ GeV). If the elementary Fermi theory were to

remain true as the energy continues to increase, then the effective strength of this "weak" interaction would continue to grow until it became stronger than both electromagnetic and strong interactions. Eventually the continued growth would clash with the principle of unitarity for purely leptonic systems at a c. m. energy of order 300 GeV. (This principle of unitarity is basic to all present understanding of elementary particle theories but has not been experimentally verified at these high energies.)

Further, from the point of view of field theory the elementary Fermi theory cannot be a fundamental theory since calculations including the higher orders are badly divergent. Nevertheless, we are faced with the experimental fact that the observed $K_1^0 - K_2^0$ mass difference is roughly second order in the Fermi constant

$$\Delta m = m_K \left[G m_K^2 \right]^2$$

and thus higher order weak interactions must be present in some fashion.

Physicists are faced here with a puzzle of the type which in the past has led to major new discoveries. A fundamental theory must fail in a region of higher energy but the nature of this breakdown is not yet known.

To answer the question, "At what energy should a deviation occur from the elementary Fermi theory?", one can appeal to the principle that the weak interaction with its inherent violation of parity and strangeness conservation should always remain smaller than the electromagnetic. If this were the case then at an energy when the electromagnetic and weak interactions are comparable some kind of effect might occur. Namely, when

$$\frac{G^2 S}{\pi} = \frac{4\pi\alpha^2}{S}$$

or $S \approx 4000 \text{ GeV}^2$. Since such a value for S falls in the region accessible to PEP weak interaction experiments will be among the most significant investigations that can be carried out at such a facility. Either the observation of the weak interaction growing in strength to surpass the electromagnetic, or a breakdown of the Fermi theory, would constitute a spectacular and important result.

The study of the weak interaction process would be via the reaction

$$ep \rightarrow \nu + \text{'anything'}$$

when the 'anything' would be composed of various combinations of hadronic, leptonic and photonic states. Since the neutrino is unobservable the determination of the important kinematic quantities, the energy and momentum transfer to the lepton system, will be made by observing the complete collection of final states. There will be a net transverse momentum imbalance of the observed final states to compensate the momentum carried off by the neutrino and thereby producing a very distinctive signal for the weak interaction events. The feasibility of this task is discussed below.

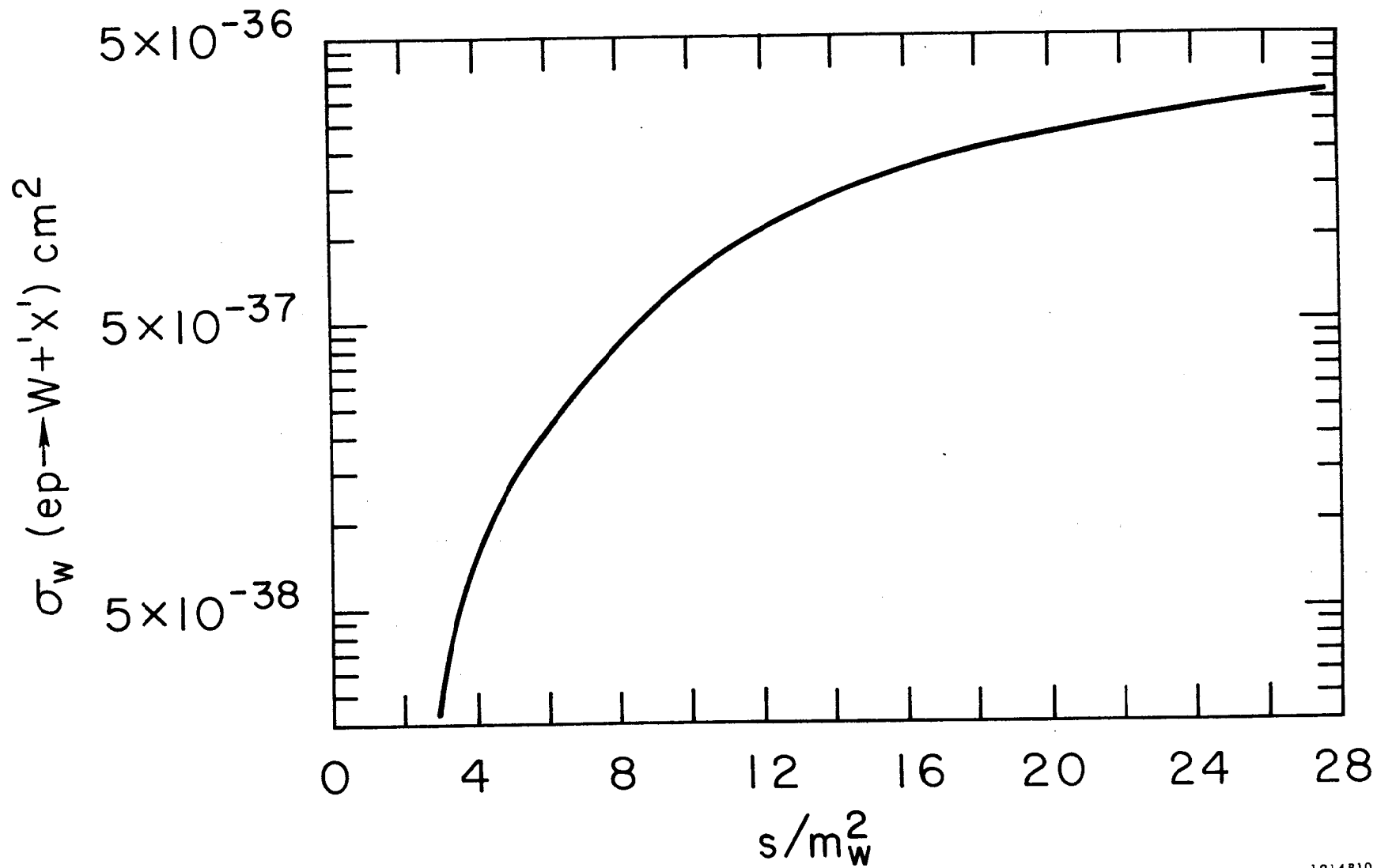
An experimental study of weak interactions might begin with first establishing whether the conventional theory which is applicable at lower energies might continue to apply. This would be to determine whether the total cross section did rise proportional to the c.m. energy squared S . Deviations from this dependence could be due to the existence of an intermediate meson W which prevents the lepton current from interacting locally with the hadron current. Or the deviation might be due to a failing of the current \times current hypothesis even in the presence of a W meson. In the first case the cross section would rise linearly with S only when S is smaller than M_W^2 . When $S > M_W^2$ these mesons could be produced in final states thus allowing for a direct measurement of their existence.

There are essentially two mechanisms for producing W particles in the final states: either as single production of one W , or by pair production of (W, \bar{W}) .

In the process $ep \rightarrow W + \text{'anything'}$ the electromagnetic and the semi-weak interaction will both occur. While in the process $ep \rightarrow W^- W^+ + \text{'anything'}$, only the electromagnetic interaction will occur. In the first case the dominant mechanism by several orders of magnitude is just the photoproduction of single W 's without neutrino emission and the cross section will be of order

$$\alpha_W = \alpha^2 G \log \frac{2E_l}{m_e} = 2 \times 10^{-36} \text{ cm}^2$$

provided $S/M_W^2 \gg 1$. Figure 1 shows the dependence of the cross section as S approaches M_W^2 . Since the W lifetime is short of order 10^{-19} sec its production would be observable only through its decay products. Observation of a single lepton at high transverse momentum via the decay mode



1914B10

FIG. 1--Total intermediate vector meson (W) production cross section in lepton-hadron collisions.

$W \rightarrow \mu(e) + \nu$ with the unobserved neutrino carrying off the missing transverse momentum would be a signal peculiar to the W production.

In the second case of W pair production the cross section is expected to be of order

$$\alpha_W \approx \frac{\alpha^4}{M_W^2} \log \frac{2E_\ell}{m_e}$$

which is in general smaller than the single W production for W masses greater than 18 GeV. However, should the W-meson have some kind of anomalous magnetic moment the above estimate would be several orders of magnitude too small. The pair production of W's would in principle be detected similarly to the case of $e^-e^+ \rightarrow W^-W^+$ by the coincidence detection of a large transverse momentum muon and electron from each of the W decays.

Tests of the existence of any current-current interactions can be made by studying the dependence of the cross section on the center-of-mass energy. The general form of $S^2 (d^2\sigma/dq^2 d\nu)$ must be at most a quadratic function of S for fixed ν and q^2 if the form of the interaction is any of the five possible tensor invariants (S, P, V, A, T) or if these invariants are made nonlocal by coupling to various intermediate mesons.

If the weak interactions of the type $ep \rightarrow \nu + \text{'anything'}$ continue to be described by the matrix element of a local current between the initial proton state and the final hadronic state 'anything' even at PEP energies, then one may envision various experimental studies relevant to the problem of nucleon structure and hadronic symmetries. We list some examples of high physics interest which would be experimentally feasible with the PEP parameters considered here. Should experiment show that the simple Fermi theory does not apply then possibly other experiments may become more significant such as the W meson production mentioned above.

Experiments Testing Conventional Weak Interaction Concepts

i) Current algebra sum rules by Adler. From the $SU_3 \times SU_3$ chiral algebra of currents Adler has shown that when the incident electron energy is large

$$\frac{d\sigma(e^- p)}{dq^2} - \frac{d\sigma(e^+ p)}{dq^2} = \frac{G^2}{2\pi} (\cos^2 \theta_c + 2 \sin^2 \theta_c)$$

and

$$\frac{d\sigma(e^- n)}{dq^2} - \frac{d\sigma(e^+ n)}{dq^2} = \frac{G^2}{2\pi} (-\cos^2 \theta_c + \sin^2 \theta_c)$$

where θ_c is the Cabibbo angle and where the various cross sections refer to the total inelastic weak process.

The inverse of these reactions with the initial lepton being neutrino or antineutrino will be studied at NAL in the c.m. energy squared (S) region of 400 - 800 GeV². Measurements at PEP would test these very basic sum rules at S values an order of magnitude higher.

Thus such assumptions as the conserved vector current hypothesis as well as the algebra of current densities will be confronted by experiment in a much higher energy domain.

ii) Measurement of the structure functions. If the hadronic matrix elements involved in the weak interaction inelastic process can be represented as matrix elements of vector and axial-vector currents as is valid at lower energies then in terms of calculated energy and momentum transfer between initial and final lepton the cross section can be written in terms of three structure functions (see Eqs. (8a or 8b), below). These functions are analogous to the structure functions of inelastic electron scattering experiments and their measurement will give added information about the structure of the nucleon and the validity of the scaling hypotheses in this new energy domain.

Many other questions about weak interactions of considerable physics interest can also be studied. These are briefly listed below.

iii) The existence of jets in the final state hadronic systems, i. e., are the secondary hadrons confined to a column with small transverse momentum about a specified direction as suggested by certain parton models?

- iv) What is the ratio of total strange to nonstrange particle production, i. e., is the Cabibbo suppression factor of $\sin \theta$ playing the same role as at lower energies?
- v) Are there diffraction processes present when the weak current has large invariant mass?
- vi) Do the hadronic multiplicities behave in a similar manner when compared to electromagnetic and strong processes?
- vii) Are there analogous scaling laws in the final state hadronic distributions in transverse and longitudinal momentum?

Although this list is far from complete, it indicates the wealth of studies that could be made in the area of conventional weak interactions with the PEP facility.

C. Experimental Considerations

In this section we discuss the kinematics, counting rates and detection problems related to the study of large momentum transfer weak and electromagnetic transfer. We conclude that the counting rates are reasonable and the experimental signatures of both the weak and electromagnetic events are sufficiently unique to allow their identification without any new developments in detector technology.

1. Kinematics¹

Neglecting the electron rest mass, the kinematics for inelastic electron scattering and neutrino production reactions are the same, and are shown in Fig. 1. The usual relation,

$$Q^2 = 2M\nu + M^2 - W^2, \quad (1)$$

with M^2 and W^2 being the initial and final hadron mass-squared remains valid provided the energy transfer, ν , is defined as,

$$\nu = \frac{\mathbf{P} \cdot \mathbf{q}}{M} = \frac{2E_e}{M} \left\{ E_e - E'_e \cos^2 \frac{\theta'_e}{2} \right\}, \quad (2)$$

$$\mathbf{q} = \mathbf{p}_e - \mathbf{p}'_e.$$

For the PEP parameters used in this report, $Q_{\max}^2 = S = 4200 \text{ GeV}^2$ and $\nu_{\max} = 2240 \text{ GeV}$. In Fig. 2a the solid parallel lines are loci of equal invariant hadron mass, while the parallel dashed lines are those of equal final lepton

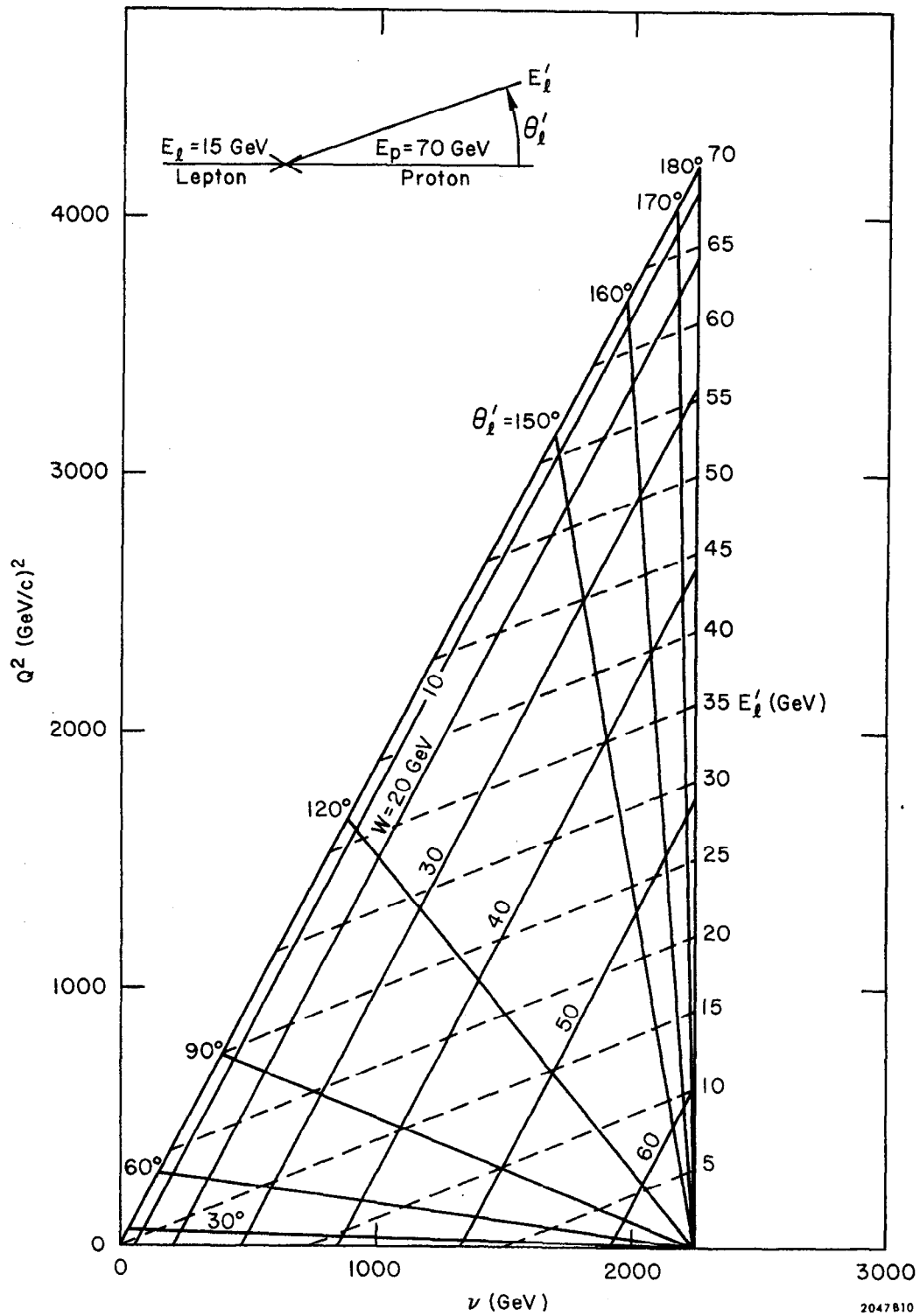


FIG. 2a--Final lepton kinematics for inelastic lepton scattering of 15 GeV leptons incident on 70 GeV protons.

energy. The radial lines originating at $\nu_{\max} = 2240$ GeV and $Q^2 = 0$ are for equal lepton scattering angles. Most of the Q^2 vs. ν space is clearly experimentally accessible. Figure 2b displays the kinematics in momentum space. Also shown are values of the scaling variables $x_1 = -u/s$, $x_2 = -t/s$ as defined by Berman, Bjorken and Kogut² where $u = -(P_p - p'_e)^2$ and $-t = Q^2$, $S = (p_e + P_p)^2$.

The distribution of final hadrons in inelastic lepton reactions either weak or electromagnetic has, as yet, not been experimentally determined. Theoretical models yield distributions ranging from jet-like distributions² of hadrons confined to the forward direction and along the direction $\vec{Q} + \vec{P}_p$ (Ref. 3) to statistical models with essentially isotropic distributions and large multiplicities. Both of these types appear to be within the limits of detectability for a PEP-type detection system.

2. Estimated Counting Rates

a. Assume structure functions continue to be functions only of $Q^2/2M\nu$

(1) Inelastic electron scattering. The usual expression for the cross section for electrons on stationary protons is,

$$\frac{d^2\sigma}{d\Omega'' dE''} = \frac{4\alpha^2 E''^2}{Q^4} \left[2W_1(\nu, Q^2) \sin^2 \frac{\theta''}{2} + W_2(\nu, Q^2) \cos^2 \frac{\theta''}{2} \right] \quad (3a)$$

where, the double primes refer to final state quantities in this frame.

The structure functions W_2 and W_1 can be expressed in terms of the photoproduction cross section by longitudinally and transversely polarized photons,

$$W_2 = \frac{1}{4\pi^2\alpha} \frac{Q^2}{\sqrt{\nu^2 + Q^2}} \left[\sigma_T(\nu, Q^2) + \sigma_L(\nu, Q^2) \right] \quad (3b)$$

$$W_1 = \frac{1}{4\pi^2\alpha} \frac{Q^2}{\sqrt{\nu^2 + Q^2}} \frac{Q^2 + \nu^2}{Q^2} \sigma_T(\nu, Q^2) . \quad (3c)$$

In the limit as $Q^2 \rightarrow 0$,

$$\sigma_L(\nu, Q^2) \rightarrow 0 ,$$

and

$$\sigma_T(\nu, Q^2) \rightarrow \sigma_\gamma(\nu) ,$$

where $\sigma_\gamma(\nu)$ is the photoproduction cross section for real photon of energy ν .

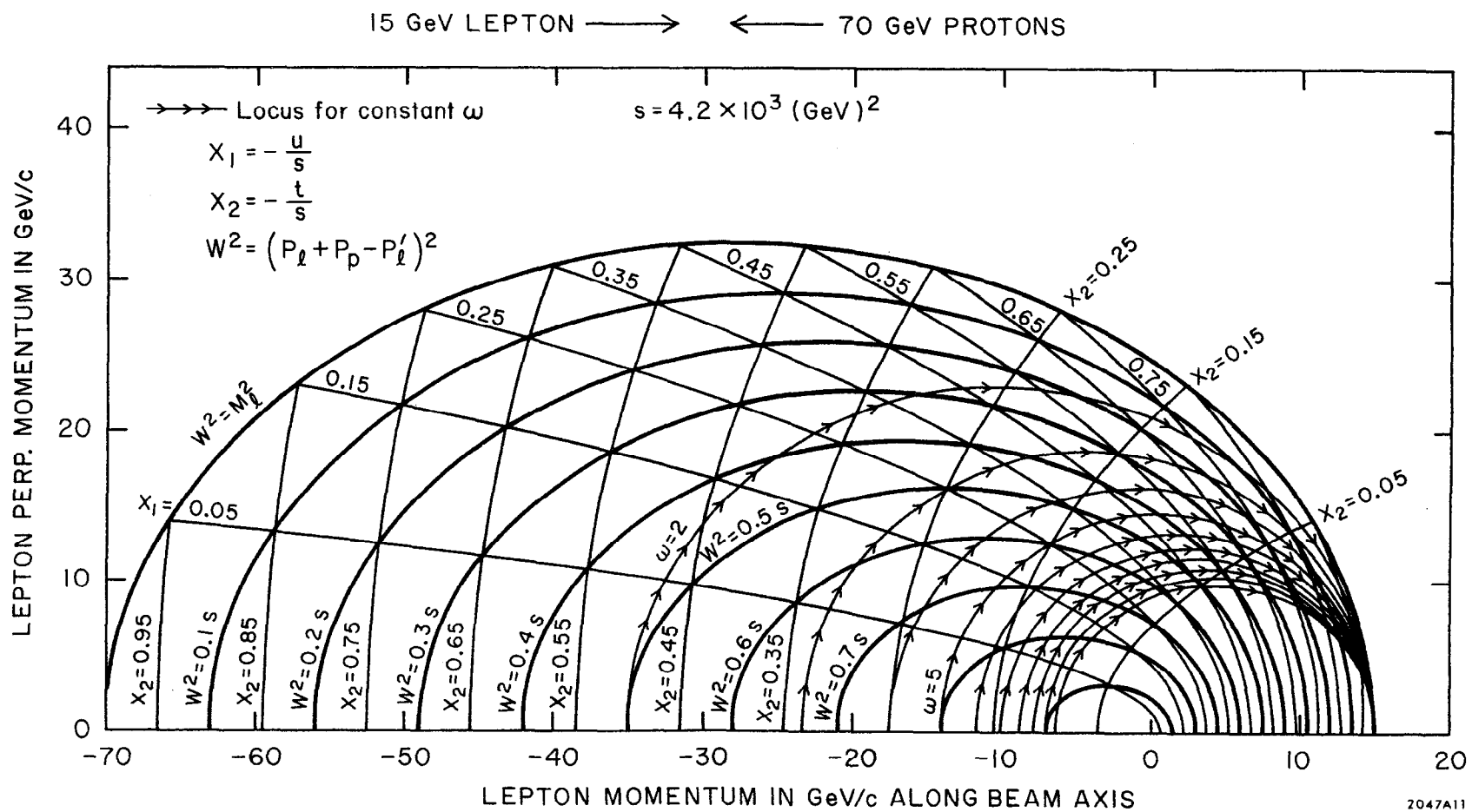


FIG. 2b--Final lepton kinematics for inelastic lepton scattering of 15 GeV leptons incident on 70 GeV protons.

The present SLAC data show that $\sigma_L \ll \sigma_T$ and consequently

$$W_1/W_2 = \frac{Q^2 + \nu^2}{Q^2} .$$

Equation (3a) re-expressed in terms of the Lorentz invariant quantities, $x \equiv Q^2/2M\nu$ and $y \equiv \nu/\nu_{\max}$ becomes, ($xy = Q^2/S$, $2M\nu_{\max} = S$).

$$\frac{d^2\sigma}{dx dy} = \frac{4\pi\alpha^2}{s} \frac{\nu W_2}{x^2 y^2} \left\{ (1-y) \left[1 - \frac{M^2 xy}{s(1-y)} \right] + \frac{2M^2}{s} xy \frac{W_1}{W_2} \right\} . \quad (4)$$

Since, $M^2/s = 2.1 \times 10^{-4}$ and $W_1 \approx (\nu^2/Q^2) W_2$ (see Ref. 2), Eq. (4) can be simplified to

$$\frac{d^2\sigma}{dx dy} = \frac{4\pi\alpha^2}{s} \frac{\nu W_2}{x^2 y^2} \left(\frac{1}{2} + \frac{1-y}{y^2} \right) \quad (5)$$

Furthermore, if the structure function νW_2 is approximated by the simple form,

$$\nu W_2 \approx \frac{1}{4} (1-x) \quad (6)$$

one has,

$$\frac{d^2\sigma}{dx dy} \approx \frac{\pi\alpha^2}{s} \left(\frac{1-x}{x^2} \right) \left(\frac{1}{2} + \frac{1-y}{y^2} \right) \quad (7)$$

Figure 3 shows the number of events detected per day in the various portions of the Q^2 vs. ν space, using,

- i. Luminosity = 10^{32} (cm² sec)⁻¹
- ii. $0.01 \leq x$ and $y \leq 1$
- iii. 100% detection efficiency.

(2) Neutrino interactions. (The final lepton is a neutrino.) The equation analogous to Eq. (5) is,

$$\frac{d^2\sigma}{dx dy} = \frac{G^2 s}{2\pi} \nu \beta \left\{ (1-y) + \frac{y^2}{2} [(R) + (L)] + y \left(1 - \frac{y}{2} \right) [(L) - (R)] \right\} \quad (8a)$$

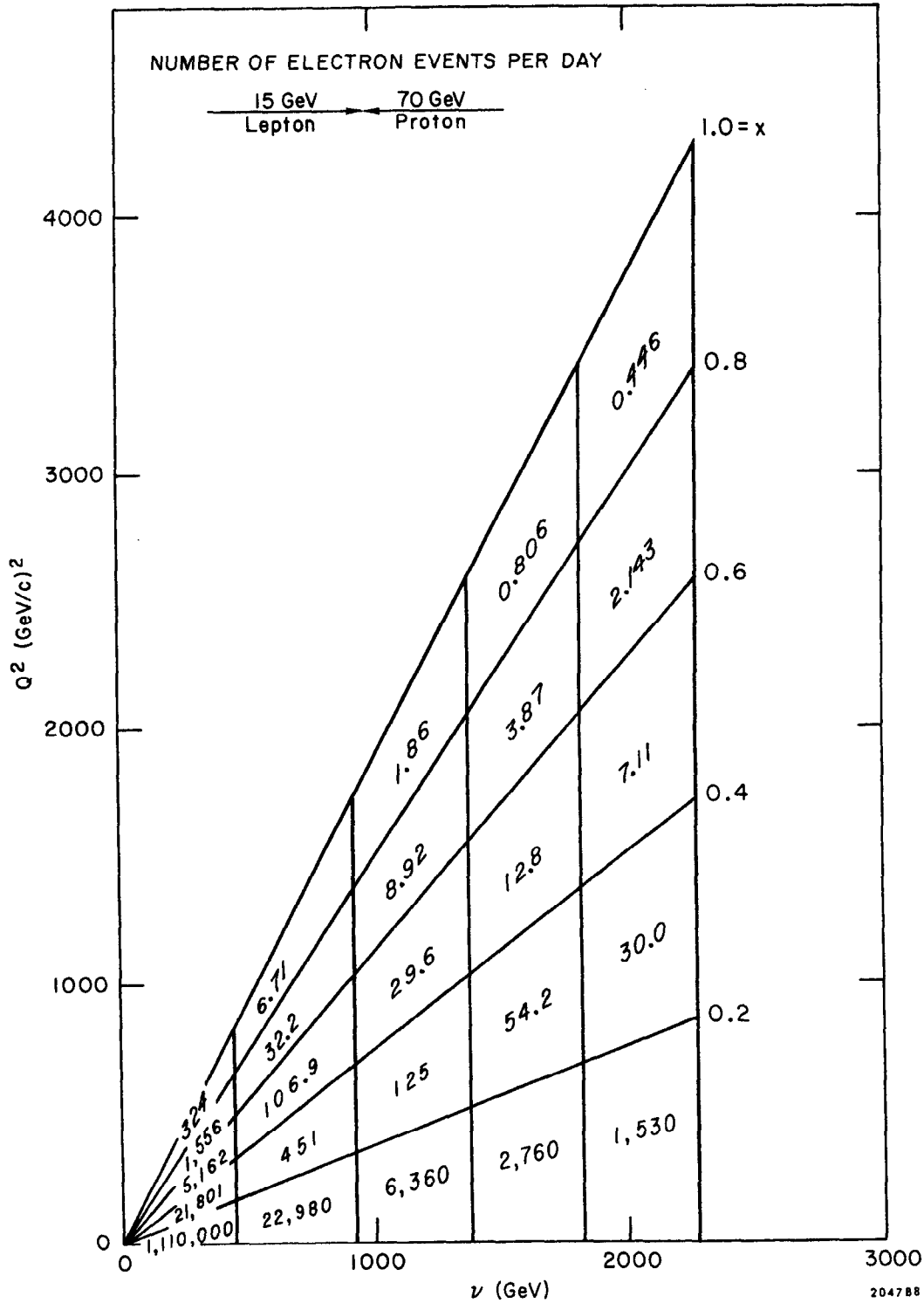


FIG. 3--Inelastic lepton scattering event rate using

$$1) \frac{d^2\sigma}{dx dy} = \frac{\pi\alpha^2}{s} \left(\frac{1-x}{x^2} \right) \left(\frac{1}{2} + \frac{1-y}{y^2} \right) \left(\text{assuming } \nu W_2 \approx \frac{1}{4}(1-x) \right)$$

$$\text{and } W_1/W_2 = \nu^2/Q^2. \quad 2) \quad 0.01 \leq x \text{ and } y \leq 1.$$

3) 100% detection eff.

4) Luminosity = $10^{32} (\text{cm}^2 \text{sec})^{-1}$.

or

$$\frac{d^2\sigma}{dx dy} = \frac{G^2 s}{2\pi} Q^2 (1-x) \left\{ \sigma_L + (1-y) \sigma_S + (1-y)^2 \sigma_R \right\} \quad (8b)$$

Where

$$\nu\beta (= \nu W_2) = \frac{Q^2}{2\pi} (1-x) (2\sigma_S + \sigma_R + \sigma_L) \quad (9)$$

$$(R) = \frac{\sigma_R}{2\sigma_S + \sigma_R + \sigma_L} \quad (10)$$

$$(L) = \frac{\sigma_L}{2\sigma_S + \sigma_R + \sigma_L} \quad (11)$$

with σ_R , σ_L , and σ_S being the 1, -1, 0 helicity cross sections.

Figure 4a shows the number of events per day in the various sectors of Q^2 and ν for the spin 1/2 parton model which states that $\sigma_R = \sigma_S = 0$. Other assumptions are:

- i. $\sigma_{TOT} = 0.8 \nu \max 10^{-38} \text{ cm}^2$
- ii. Luminosity = $10^{32} (\text{cm}^2 \text{ sec})^{-1}$
- iii. $\nu\beta \propto (1-x)$
- iv. 100% detection efficiency.

Comparing Fig. 3 with 4 at the largest Q^2 one finds that the weak interactions are comparable in counting rate to the electromagnetic ones.

b. What kinds of things are measurable with these rates?

A ten day run seems a reasonable period of time. A 100 day run is very long and begins to approach the length of runs anticipated at NAL for neutrino bubble chamber exposures. A 1000 day run is completely out of the question. We therefore, adopt arbitrarily (a) a maximum run duration of 100 days, as a way of determining the minimum acceptable luminosity, (b) the average duration of a run is 10 days.

(1) The separate determination σ_L , σ_S and σ_R as a function of x and y can be accomplished by exploiting the differences in y dependence of the factors 1, $(1-y)$, and $(1-y)^2$, respectively of Eq. (8b). Figure 5 shows that the similarity of the $1-y$ and $(1-y)^2$ will cause some difficulty in separating

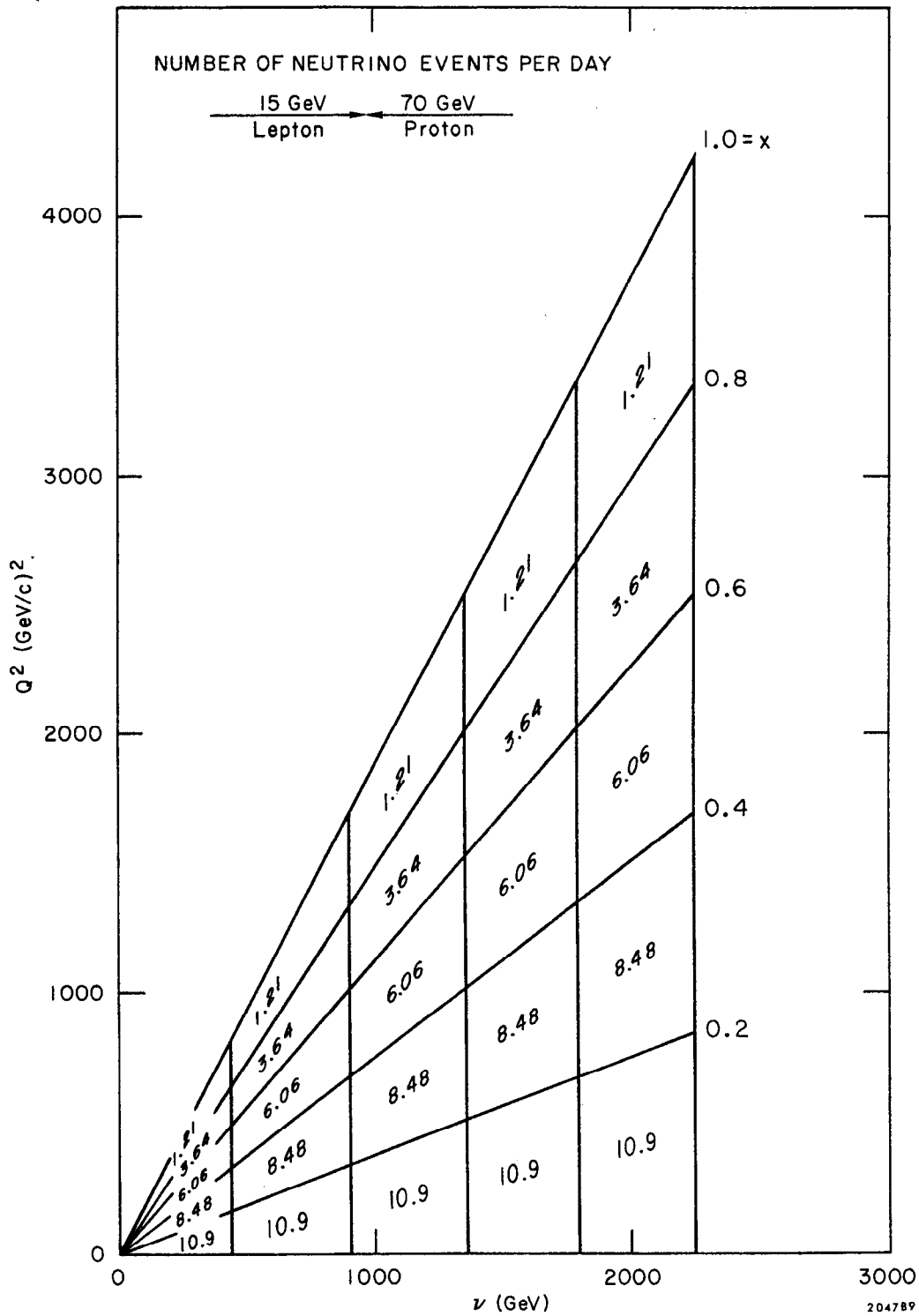


FIG. 4--Neutrino event rate for spin 1/2 parton model assuming

- 1) $\sigma_{\nu n} = 0.8 \nu_{\max}^{-1} 10^{-38} \text{ cm}^2$. 2) $\nu (\beta \equiv \frac{W_2}{2}) \propto (1-x)$.
- 3) $\sigma_R = \sigma_S = 0$, i.e., spin 1/2 parton model.
- 4) 100% detection eff. 5) Luminosity = $10^{32} (\text{cm}^2 \text{ sec})^{-1}$.

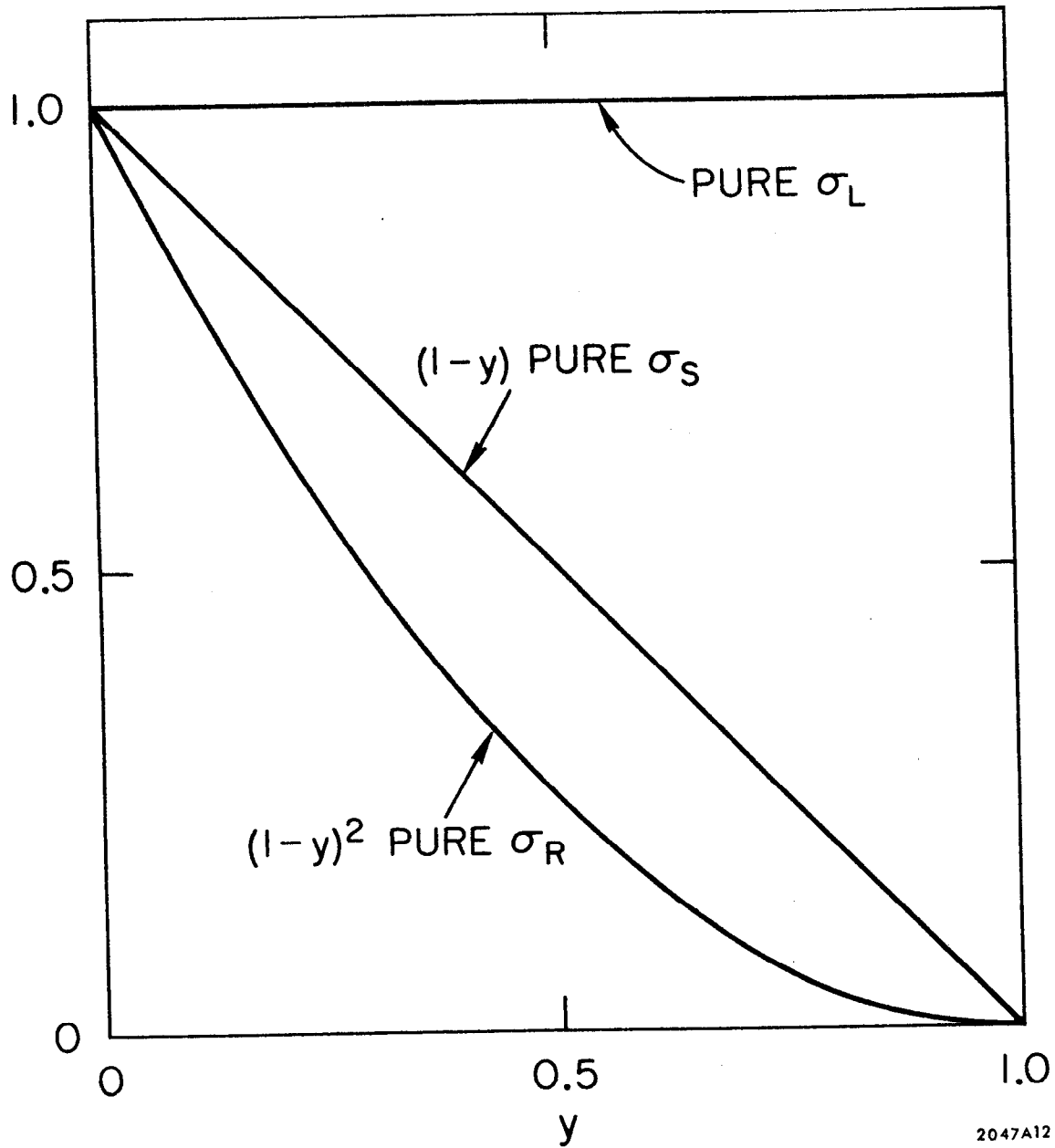


FIG. 5--The kinematic y dependence of the factors in front of σ_L , σ_S and σ_R as defined in Eq. (8b).

σ_S from σ_R . Because the factor 1 is much different from the others indicates that σ_L can be easily measured separately from σ_S and σ_R .

(2) Modification of "scaling" by the intermediate vector boson (IVB). The presence of an IVB would cause $G^2/2\pi$ to be replaced by $(G^2/2\pi) \left[\frac{M_W^2}{(M_W^2+Q^2)} \right]^2$. Figure 6 shows the distortion factor $\left[\frac{M_W^2}{(M_W^2+Q^2)} \right]^2$ as well as how the $\nu\beta$ structure function would be modified as a function of y by the presence of an IVB of mass $M_W = 53$ GeV. The error bars represent the statistical uncertainty that would result from a 10 day run on PEP. Only the data between $0 < y < 0.2$ (labelled as $y = 0.1$) and $0.8 < y < 1.0$ (labelled as $y = 0.9$) have been plotted. The remaining data between $0.2 < y < 0.8$ yield additional information. It is evident from this figure that in a ten day run one could clearly observe the effects of an IVB as massive as 50 GeV. If the luminosity were $10^{31} \text{ (cm}^2 \text{ sec)}^{-1}$ this run would have to be 100 days, the maximum tolerated by our criteria.

(3) Enhancement of inelastic electron scattering by an neutral intermediate boson, a form of breakdown of scaling.⁴ Can one observe effects caused by very massive intermediate bosons? As a guide to answering this question we choose the Weinberg⁵ model as an example. It calls for an intermediate scalar boson of mass M_ϕ as well as an intermediate vector boson of mass M_W and an intermediate neutral boson of mass M_Z .

The interference of the massless photon amplitude with that of the intermediate neutral boson amplitude produces a detectable term. Adding this interference term to Eq. (5) yields,

$$\frac{d^2\sigma}{dx dy} = \frac{4\pi\alpha^2}{s} \frac{\nu W_2}{x^2} \left(\frac{1}{2} + \frac{1-y}{y^2} \right) \left\{ 1 + 2 \left(\frac{e_Z}{e} \right)^2 \frac{1}{1 + \frac{m_Z^2}{s} \frac{1}{xy}} \right\}, \quad (12)$$

where

$$\frac{e_Z}{e} = \frac{3}{4} \tan \theta_W - \frac{1}{4} \cot \theta_W; \quad (13)$$

θ_W is the Weinberg angle defined as $\tan \theta_W = g'/g$, the ratio of the (NIB) and (IVB) coupling constants.

$$m_W = 37.3 \text{ GeV} / \sin \theta_W, \quad \text{and} \quad m_Z = 2(37.3) / \sin 2 \theta_W.$$

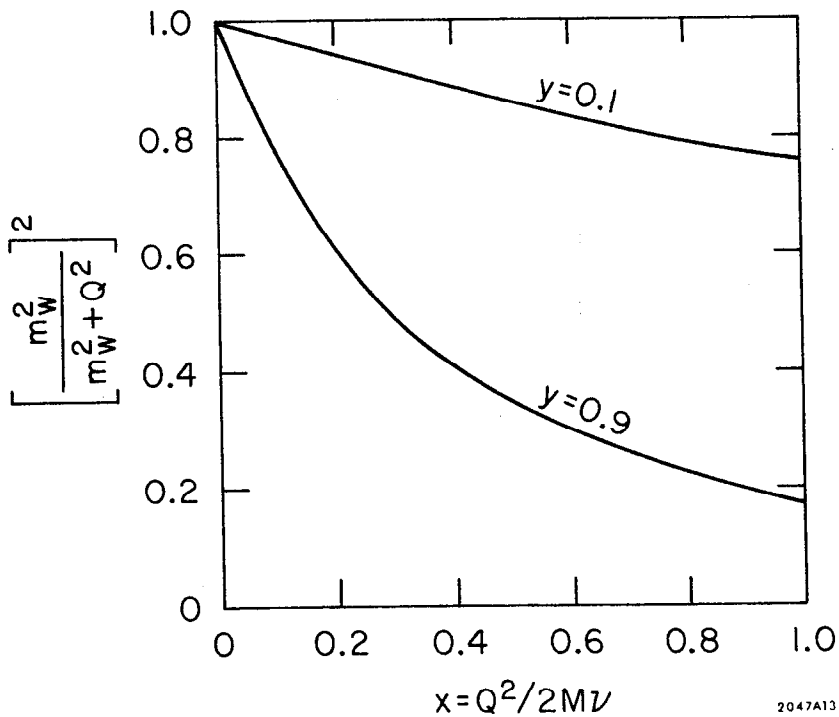
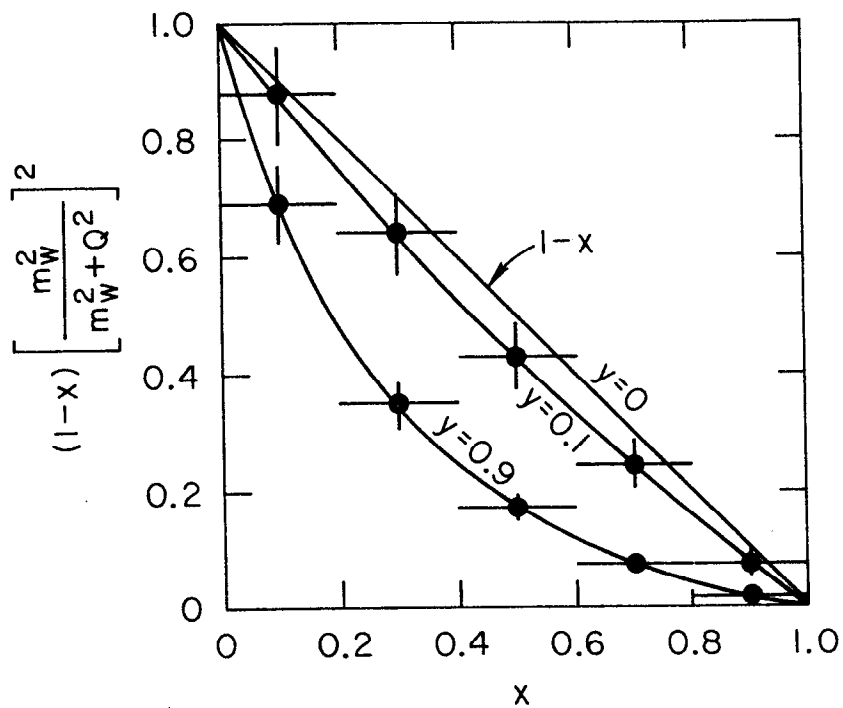


FIG. 6--How scaling for neutrino events would be broken by the existence of 53 GeV intermediate vector boson. Error bars correspond to a 10 day run. The variable $x = Q^2/2M\nu$; $y = \nu/\nu_{\max}$.

The quantity in brackets $\{ \}$ in Eq. (12) is defined as the "enhancement factor" and is plotted vs. x and y in Fig. 7 for two different values of θ_w , namely, $\theta_w = 0$ and 90 degrees. The "daisies" emerging from the square plots are typical statistical errors in the enhancement factor that would result in a ten day run. For the $\theta_w = 90^\circ$ case it is clearly a detectable effect. For $\theta_w = 0$ it is doubtful. Reformulated in terms of minimum acceptable luminosity, $\mathcal{L}_{\min} = 10^{31} (\text{cm}^2 \text{sec})^{-1}$ for $\theta_w = 90^\circ$ and $\mathcal{L}_{\min} \approx 10^{32} (\text{cm}^2 \text{sec})^{-1}$ for $\theta_w = 0^\circ$.

c. Detector requirements

We consider in this section the detector requirements for the study of both the deep inelastic electron scattering and the weak interaction. In the deep inelastic scattering region, the electromagnetic event rate is expected to be comparable to the weak interaction event rate.

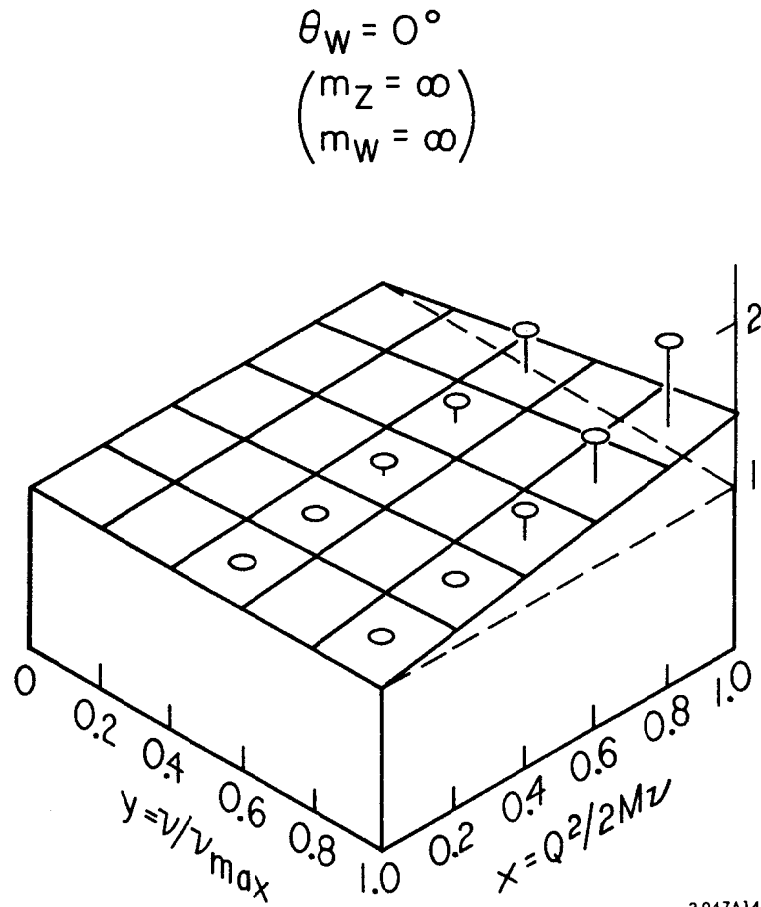
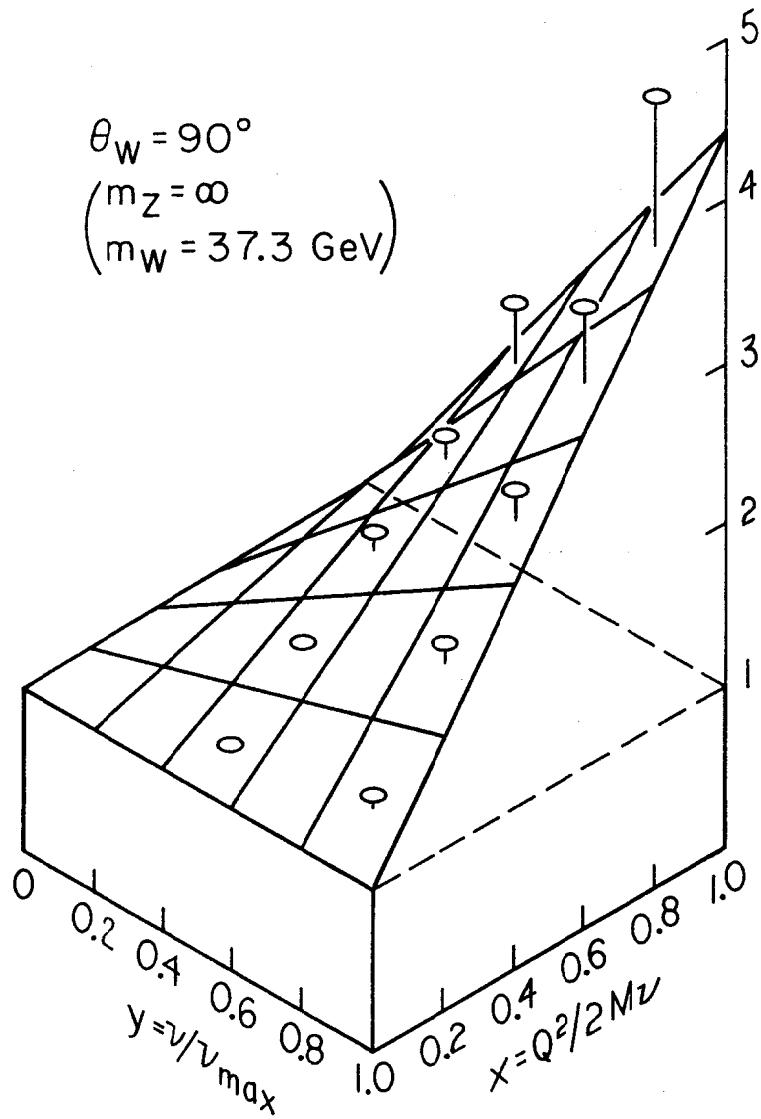
Identification of the inelastic electron scattering processes is a fairly simple affair experimentally. The kinematics shown in Fig. 2a, b indicates that over almost all of available Q^2 and ν space, a high energy secondary electron is produced at a relatively large angle to the beam line. The use of the well developed shower counter technique allows the unambiguous identification of an electron even in a large background of other particles.

Identification of a weak interaction process is a more subtle problem. The signature used to identify a weak reaction will be the absence of an electron in the final state:

$$e^\pm N \rightarrow \nu_e + X .$$

In this reaction, $N = n$ or p , and X is the net hadronic final state. The characteristic signature which must be recognized is the large energy-momentum unbalance caused by the neutrino, which escapes detection; this is in contrast to the E. M. case, where all particles, including the electron, are detectable, and within the resolution of the detector a balance of momentum-energy is observed.

This then imposes the crucial requirements upon the detector: (1) It should be able to measure energy and directions of all hadrons with "good" precision; (2) it must not fail to detect electrons with any appreciable probability, and (3) it must cover essentially the 4π solid angle. These requirements can be satisfied using present day techniques.



2047A14

FIG. 7--How scaling for electron events would be broken by the existence of a neutral intermediate boson of the Weinberg type for $\theta_W = 0$ and 90 degrees. Error bars are typical of those for a 10 day run at PEP with $\mathcal{L} = 10^{32} \text{ (cm}^2 \text{ sec)}^{-1}$.

(1) Electron detection and measurement. A relatively inexpensive, high efficiency electron shower detector (ESD) can be made of alternate layers of lead and plastic scintillator perhaps 10 radiation lengths thick, with enough layers to insure that the statistics of shower formation do not limit the counter resolution. Such a detector is currently being built at LBL for use at SPEAR. This type of detector can be made essentially 100% efficient for detecting electrons in the 1-2 GeV range; furthermore, its relative resolution improves with energy as: $\Delta E/E \sim 1/\sqrt{E}$. Thus, at PEP energies it should work very well indeed. The plan for a PEP detector might be similar with perhaps 10 radiation lengths and 10 - 15 planes. Proportional wire spark chambers are also to be located at different depths to give directly the shower location and hence the direction of the electron (or γ -ray) which initiated the shower.

(2) Hadron measurement. A more difficult problem is the one of measuring the hadrons. This would be accomplished by a large calorimeter lying behind the electron detector.⁶ The scale of the hadron showers is 20 - 30 times longer than that of the electron shower, and somewhat poorer resolutions must be expected. One may expect that techniques of calorimetry will improve, since they have been only slightly explored or used at present. By means of a modular type of design with wire chambers it appears straightforward to measure energies and directions of individual hadrons. The calorimeter also does the work of a muon identifier by measuring the multiple scattering of the muon through several interaction lengths of material. Recent work in this area shows promise of doing efficient separation based upon multiple scattering.⁷

(3) Reconstruction of event. In the case of an e^-p event, a large missing momentum and energy transverse to the beam pipe and absence of an electron pulse from the ESD is the signature for a missing neutrino. If there is relatively little missing transverse momentum, then the absence of a large pulse in the ESD might be explained by an electron from an EM event going forward down the beam pipe. How large the P_T unbalance must be to give a certain identification is of course a function of the background level and the calorimeter resolution.

It is noted that this criteria makes use of a minimum P_T missing relative to the beam direction, and automatically this criteria simultaneously insures that the EM background is suppressed by requiring a corresponding minimum Q^2 .

(4) The need for a magnetic field. Up until now no mention has been made of possible momentum measurement by a magnetic field. This is because the identification of the WI events have not required it. Rather, in fact, the identification depends mostly on adequate measurement of the highest energy particles, which are likely to be the most poorly measured in a magnetic field and the best measured in a calorimeter. However, considering the possibly large hadron multiplicities, one should use all means possible to sort out the resulting confusion. The SLAC experimenters' ability to reverse the magnet polarities on their spectrometers allows them to measure the positron of the Dalitz pair, thereby, allowing them to subtract out the Dalitz pair background. In similar fashion a magnetic field would be useful in eliminating the same background in PEP.

It is therefore highly desirable to have a magnetic field, at least to be able to determine sign-of-charge of all particles. To all these necessary components are added now inner wire chambers to read out coordinates of charged tracks for the reconstruction of the events, including a proportional wire chamber (PWC) surrounding the beam pipe interaction region which is essential in reducing the cosmic ray trigger rate. Several other such PWC's at small radius may also provide for detection of Λ and K_S^0 decays.

References

1. See for example "Inelastic electron-proton scattering with SPEAR plus a proton ring," M. L. Stevenson PEP-Note 3 (13 October 1971).
2. S. Berman, J. Bjorken, and J. Kogut, "Inclusive processes at high transverse momentum, (Report No. SLAC-PUB-944 (August 1971)).
3. G. Goldhaber, "Additional remarks on the reaction of the type $ep \rightarrow e'\rho N^*$," PEP-Note 17 (17 February 1972).
4. M. L. Stevenson, "The kinematics and possible dynamics of inelastic lepton scattering in PEP," PEP-Note 16 (10 February 1972).
5. S. Weinberg, Phys. Rev. Letters 19, 1264 (1967) and Phys. Rev. Letters 27, 1688 (1971).
6. See for example S. Wojcicki, "Calorimetry for weak interaction experiments at PEP," WI PEP memo No. 7.
7. S. Parker, WI PEP memo No. 9.

III. PHOTOPRODUCTION (ALMOST REAL PHOTONS)

A. Introduction

Electrons scattered in the Coulomb field of the incoming proton will produce an effective spectrum of photons for interaction with this proton. The energy of these photons is just the energy lost by the scattered electron.

If the scattered electron is confined to the exact forward direction, then in the limit of negligible electron mass, the photons interacting with the proton will have their energy equal to their momentum. This situation of zero mass corresponds to the usual case of a photon beam scattering on a proton target, except that in PEP the proton is also moving in the laboratory system toward the photons with very high momentum. This makes it possible to extend the investigation of photoproduction processes to a very much higher energy regime.

For most photoproduction reactions one would like to measure the energy dependence of the process. In principle this can be accomplished either by a subtraction of measurements at two slightly different incident electron energies or by using a "tagged" photon beam in which the photon energy is determined from a coincidence measurement of the scattered electron. Given the expected luminosity of $10^{32} \text{ cm}^{-2} \text{ sec}^{-1}$ and our present knowledge of photon cross sections, the subtraction method would yield insufficient counting rates. Thus a knowledge of the photon energy requires a tagged beam.

In this connection one encounters the very important problem of bremsstrahlung by the beam electron. Electrons which have lost energy by this process can be confused with the electrons involved in hadronic reactions, and are produced at such a large rate that they would completely swamp any detector designed to measure an electron at zero degrees in coincidence with a hadron. Fortunately the bremsstrahlung cross section falls very rapidly with angle, while the hadronic reactions fall much more slowly. Thus it is possible to choose an angular range for the detected electron in which the bremsstrahlung contribution is negligible, but in which the photon mass is still small enough to be neglected and the photon can be considered real for the hadronic processes we wish to study.

B. Physics of Photoproduction

The availability of a high energy photon beam at PEP allows for the study of photon-induced reactions up to an equivalent laboratory system photon energy of 2250 GeV. This allows for the extension of present photoproduction experiments to a much higher energy domain, as well as the study of new processes that are available only for study because of the much larger c.m. energy.

Examples of the first type are:

- (a) Total hadronic γP cross sections,
- (b) Specific two-body and quasi-two-body states, such as $\gamma P \rightarrow \rho^0 P, \phi^0 P; \gamma p \rightarrow \pi^+ n, \gamma P \rightarrow \gamma p,$
- (c) Inclusive reactions $\gamma P \rightarrow h + \text{anything}$, where h is an observed hadron or photon,
- (d) Certain tests of QED,
- (e) Production of multibody final states.

Examples of the second type are:

- (f) W-meson production: $\gamma P \rightarrow W^- W^+ + \text{anything}$,
- (g) Heavy lepton or quark pair production.

We discuss these processes below in light of their physics interest.

Total hadronic γP cross sections

Here one expects the energy dependence of the cross sections to follow that of purely hadronic total cross sections. At laboratory system energies of order 20 GeV, the γP cross section is known to be approximately constant in energy and of amount 120 μb . Experiments detecting the produced hadrons should be able to determine a possible $\log s$ (\sqrt{s} is the γP c.m. energy) dependence in the energy variation of the cross section to about a 5% accuracy. Any deviations of the energy dependence of the total γP cross section from the hadronic cross section behavior would be totally unexpected and thus this measurement constitutes an important check on the general understanding of strong and electromagnetic reactions. Since the ISR will have measured hadronic total cross sections to a center-of-mass energy of 50 GeV, PEP measurements up to c.m. energies of 65 GeV would lead to comparisons in the same general energy region. Furthermore, we note that the γP total cross section serves as input into the calculation of the Compton scattering amplitude via the method of dispersion relations and thus its knowledge is important in

connection with testing certain fundamental assumptions related to dispersion theory.

Two-body and quasi-two-body reactions

At energies of order 20 GeV, the process $\gamma P \rightarrow \rho^0 P$ is diffractive independent of energy, and accounts for about 10% of the total cross section. The higher energy photons would allow for diffractively produced heavier vector mesons ($\rho^{0'}$) possibly up to mass 17 GeV. Such heavier vector mesons have been proposed in many contexts and are a subject of considerable controversy.

Two-body processes like $\gamma P \rightarrow \pi^+ N$ and $\gamma P \rightarrow \pi^0 P$ are expected to fall as E_γ^{-2} , and if this is the case, even at PEP energies these will be very small cross sections. The interest in these processes is both in their energy dependence and in their t (momentum transfer) dependence, particularly in the very small t range. For example, the forward $\pi^+ N$ cross section multiplied by S^2 is constant and given by the Born approximation over the entire range of energies from less than a GeV up to energies of order 20 GeV.

Knowledge of the Compton process $\gamma P \rightarrow \gamma P$ is useful for the comparison of experiment with fundamental dispersion relations as well as with such models as vector dominance. Accurate measurements of the forward amplitude will give information about its real and imaginary parts which are related through dispersion relations. Since these relations are fundamental to almost all theories of elementary particles, tests of their validity are important.

The t dependence of the Compton process in the diffraction region is expected to be roughly the same as in hadronic reactions. This is indeed the case at energies of order 20 GeV, and should be tested at higher energies.

Inclusive processes $\gamma P \rightarrow h + \text{anything}$

In these processes, the comparison of the observed hadron or photon spectra with the hadronically induced spectra will yield complementary knowledge about the nature of inclusive processes. For example, at large transverse momentum p_\perp a parton model predicts a power-law dependence rather than an exponential falloff with p_\perp as observed presently at small transverse momentum.

Tests of QED

As an example, we have the muon pair production process $\gamma P \rightarrow \mu^- \mu^+ P$, where one of the muons is observed at an energy very near the photon. In this case, the virtual muon propagator in the Bethe-Heitler amplitude is removed sufficiently from its mass shell so that QED could be tested down to a range of 5×10^{-17} cm. This distance is nearly two orders of magnitude smaller than present high energy muon comparisons with the predictions of QED.

Multibody channels

Multiparticle production by photons would again be compared with the equivalent hadron processes giving complementary knowledge about the nature of the produced spectra. Here one would like to study such effects as jets emerging at large energies and transverse momenta, as predicted by parton models.

W-meson production

If the hypothesized mediator of the weak interaction (W) should exist with its mass in the range of PEP energies, then there is possibility of producing this particle by the reactions

$$\begin{array}{l} \text{(i)} \quad \text{or} \quad \left. \begin{array}{l} \gamma P \rightarrow W^- W^+ P \\ W^- W^+ \text{ anything} \end{array} \right\} \text{W pairs} \\ \\ \text{(ii)} \quad \gamma P \rightarrow W + \text{anything} \} \text{single-W production} \end{array}$$

If the W mass is greater than 10 GeV, the second process of single-W production is expected to be of order $\alpha G \sim 10^{-34} \text{ cm}^2$ for $S/M_W^2 \gg 1$, and larger than the purely electrodynamic cross section, α^3/M_W^2 , for process (i).

The process might be observed via the leptonic decay mode of the W, in which case reaction (ii) could lead to single muons or electrons with a large transverse momentum imbalance (the missing transverse momentum being carried off by the unobservable neutrino).

Heavy lepton or quark pair production

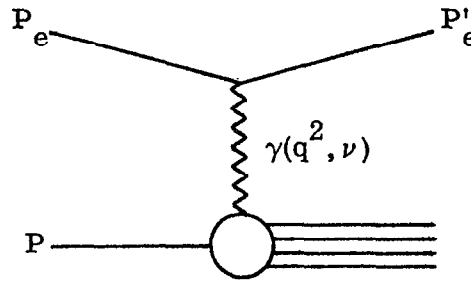
Since any charged particle interacts with photons it will be pair-produced by reactions of the type

$$\gamma P \rightarrow l^- l^+ P$$

This will allow a more definitive determination of the existence of such particles and of their possible structure.

C. Calculations of Counting Rates

For small photon momentum transfer in inelastic electron-proton scattering, the process can be considered as the radiation of an almost real photon followed by the interaction of this photon with the proton.



The Weiszacker-Williams approximation then gives the equivalent photon beam intensity coming from this small momentum transfer scattering. This can be written in terms of an equivalent radiator (X_e), where the effective bremsstrahlung intensity per electron is

$$I_\gamma = X_e \frac{dk}{k} . \quad (1)$$

This equivalent radiator is conceptually as follows. Let n be the number of hadronic reactions produced by a beam containing N electrons passing through a very small H_2 target. The equivalent radiator is defined as that fraction of a radiation length which, if traversed by the beam containing N electrons, produces a bremsstrahlung beam which, when incident on the very same small H_2 target, produces n hadronic reactions. In other words, it is the ratio of the electroproduction cross section to the photoproduction cross section. In the proton rest frame $P_e \approx 2250 \text{ GeV}/c$. The following table gives X_e for

various values of P'_e , the scattered electron momentum:

P'_e	X_e	k
0.1 P_e	3.1×10^{-2}	2025 GeV
0.3 P_e	3.7×10^{-2}	1575 GeV
0.5 P_e	4.3×10^{-2}	1125 GeV
0.7 P_e	5.3×10^{-2}	675 GeV
0.9 P_e	6.3×10^{-2}	225 GeV

We see that X_e is a function of energy and at 0.5 P_e is about 0.03. The yield for a photoproduction reaction with cross section σ_γ is then given by

$$Y = \mathcal{L} X_e \frac{dk}{k} \sigma_\gamma \quad . \quad (2)$$

To better understand the kinematics in this photoproduction region, we show in Fig. 1 plots of the momentum transfer q^2 against the laboratory electron scattering angle for several values of the final electron energy we see that for $q^2 < m_\pi^2 = 0.02$, all the scattered electrons of interest are contained within a 35 mrad cone about the electron beam. In order to know precisely the energy of the virtual photon, one must measure the energy and angle of the scattered electron (tagging). Alternatively, if one doesn't detect the scattered electron, one integrates over the entire bremsstrahlung spectrum and this procedure may be acceptable for some experiments. To enable tagging counters to miss the beam, we arbitrarily set a lower limit of 10 mrad for the angular acceptance of the scattered electron. The actual value will depend on the ultimate machine parameters.

The kinematic variables used will refer to three frames defined as follows:

	proton	electron	notation for momenta
Lab	70 GeV → (p_1)	15 GeV ← (p_2)	p
C.M. (center- of-mass)	32.5 GeV → p'_1	32.5 GeV ← $p'_2 = p'_1$	p'

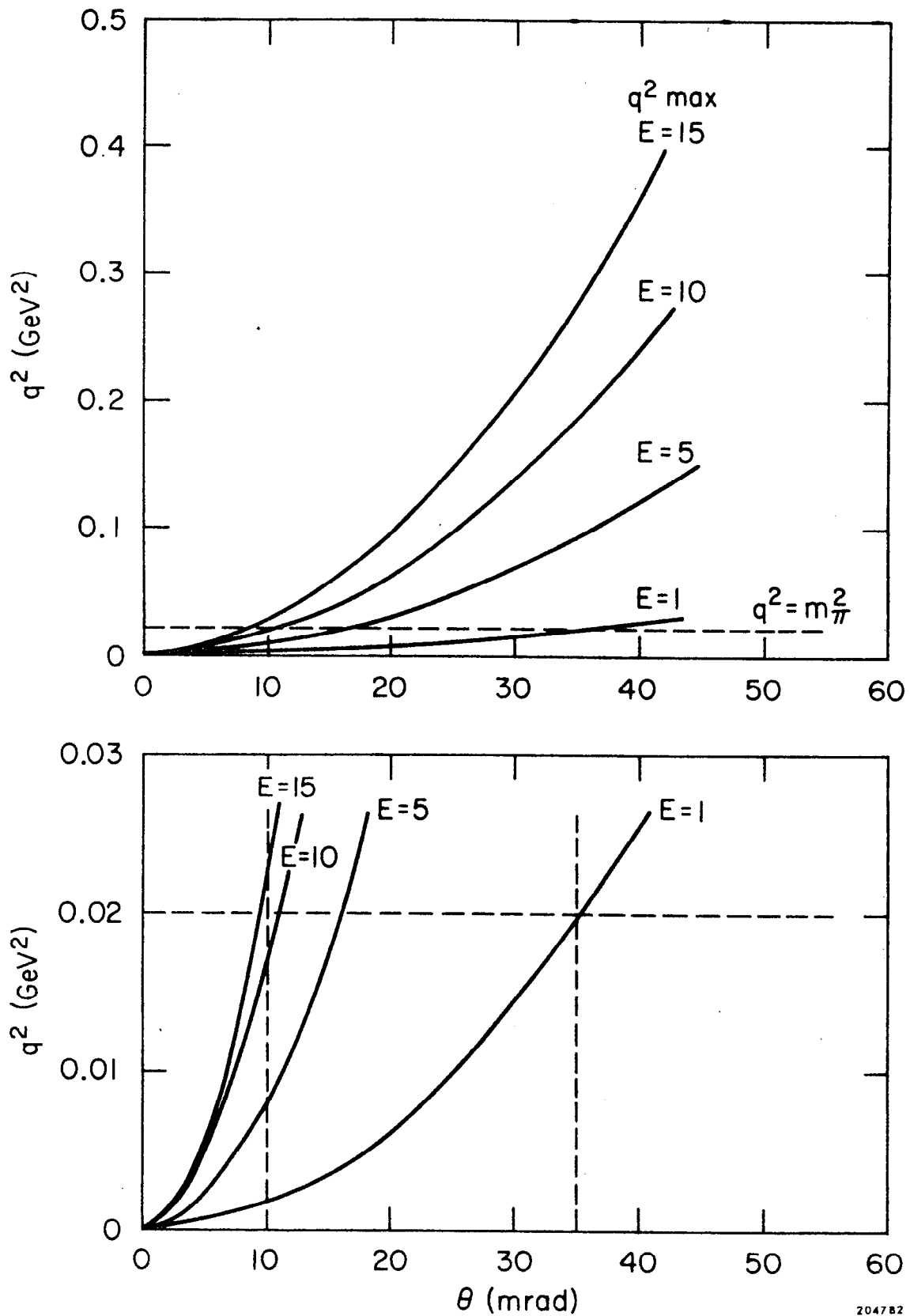
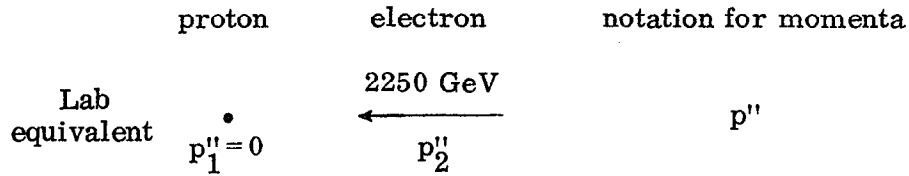


FIG. 1--Graphs of the electron momentum transfer $|q^2|$ versus the lab scattering angle in mrad for various final electron energies.



The Lorentz transformation parameters are:

between lab and c.m. $\beta_1 = \frac{p_1 - p_2}{p_1 + p_2}$ $\gamma_1 = \frac{p_1 + p_2}{2\sqrt{p_1 p_2}}$

between lab equivalent
and lab $\beta_2 = \frac{p_1}{E_1} = 1 - \frac{M_p^2}{2p_1^2}$ $\gamma_2 = \frac{p_1}{M_p}$

while the total c.m. energy squared is

$$s \approx 4p_1 p_2$$

Assuming the transverse matrix elements are independent of q^2 for (very) small q^2 , the electroproduction cross section can be written in the lab frame as:

$$\frac{d\sigma}{dE} = \frac{\alpha}{2\pi} \frac{E_0^2 + E^2}{E_0 - E} \frac{\sigma_T}{E_0^2} \ln \frac{\theta_{\max}^2}{\theta_{\min}^2},$$

where E_0, E are the incident, scattered electron energies. θ_{\min} and θ_{\max} define the angular range of detection for the scattered electron. Figure 2 shows the variation of $\frac{d\sigma}{dE}(E)$ with the following parameters:

$$E_0 = 15 \text{ GeV} \quad \theta_{\min} = 10 \text{ mrad} \quad \theta_{\max} = 35 \text{ mrad} \quad \sigma_T = 100 \mu\text{b}$$

When integrated over scattered-electron energies between 1 and 14 GeV, a total electroproduction cross section of $1.4 \mu\text{b}$ is obtained. This is approximately 1% of the total cross section for real photons so that the equivalent luminosity for tagged photoproduction is 1% of the luminosity of the storage ring. For experiments not requiring the knowledge of the photon energy we can integrate over all angles resulting in an equivalent luminosity of about 7% of the e-p luminosity.

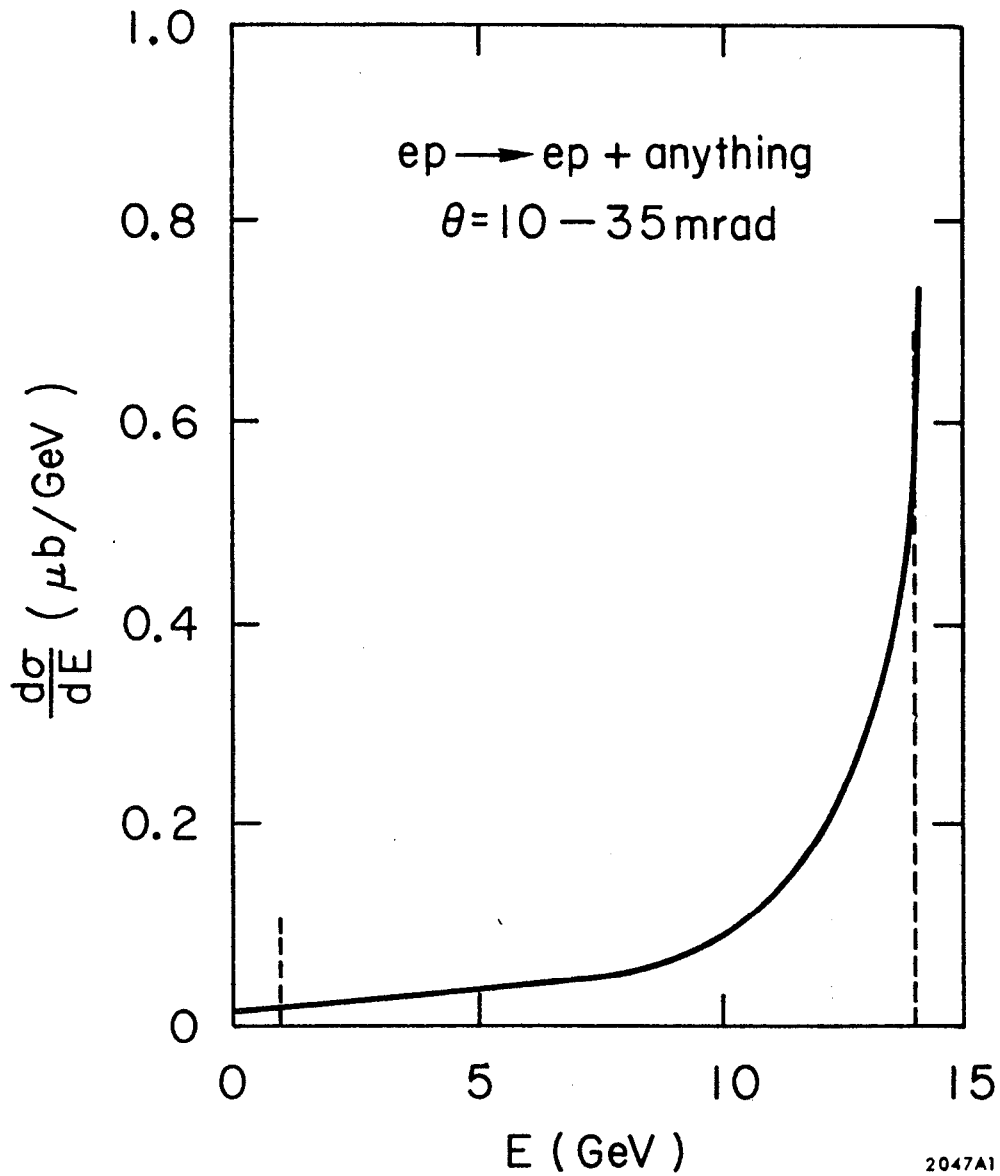


FIG. 2--Variation of $d\sigma/dE$ as a function of the final electron energy E for incident energy $E_0 = 15$ GeV, minimum angle of detection $\theta_{\min} = 10$ mrad and maximum detection angle 35 mrad with $\sigma_T = 100 \mu\text{b}$.

The following table summarizes these photoproduction luminosities, including a comparison with NAL projections.

Accelerator	Energy Range (lab equivalent)	Luminosity $\text{cm}^{-2} \text{sec}^{-1}$
NAL	150-200	3×10^{29} (tagged)
		3×10^{32} (untagged)
PEP	1500-2100	10^{29} (tagged)
		10^{30} (untagged)
PEP	150-2100	10^{30} (tagged)
		10^{31} (untagged)

Given that most experiments will require tagged photons, we can consider the backgrounds in the tagging counters from other processes.

Bremsstrahlung

In the lab equivalent frame the scattered electrons are distributed as $dE''/(E''-E')$ at angles typically $\sim m_e/E''$. The cross section in the lab frame will be:

$$d\sigma \simeq 40 \text{ mb} \times \frac{dE}{E_0 - E} = 40 \frac{dE}{\Delta E}$$

With a luminosity $\mathcal{L} = 10^{32} \text{ cm}^2/\text{sec}$ there are $20 \frac{dE}{\Delta E}$ bremsstrahlung events/crossing. Fortunately they occur at scattering angles $\theta \simeq 2\gamma_2$, $\theta'' \simeq 150 m_e/E'' \simeq 30 \mu\text{rad}$ and so the resultant electrons go straight down the beam pipe.

Pair production (tridents)

The cross section is of order 7% of the bremsstrahlung cross section and is also peaked at very small angles.

Elastic scattering

The elastically scattered electron momentum slowly increases with angle as

$$p = 15 (1 + 1.03 \times 10^{-3} q^2) \text{ GeV}/c$$

and the cross section is:

$$\frac{d\sigma}{dq^2} = 270 \frac{1 + 2.2 q^2}{q^4 (1 + 1.4 q^2)^4} \mu\text{b}/\text{GeV}^2 ,$$

giving $10 \mu\text{b}$ in the angular range 10 to 35 mrad. This is 7 times larger than the electroproduction cross section but in this case the electron energy stays equal to 15 GeV for all practical purposes; hence elastic scattering can be discriminated against when triggering a detector.

Although it is premature to discuss the actual design of the above experiments, some general-purpose detectors are envisioned. A large class of experiments will require the use of a forward spectrometer to analyze both the scattered electron and forward-produced hadrons: this setup would be particularly useful for pseudoscalar and vector meson photoproduction. Total cross section and inclusive-reaction measurements would be done with an almost 4π detector together with the tagging spectrometer. Specific experiments like Compton scattering will demand a proton spectrometer.

Table I then summarizes several classes of experiments with their typical rates.

Table I

Brief Summary of Sample Photoproduction Experiments

Process	Electron detected?	Expected cross section	Expected rate
(1) γp total cross section	yes	$120\mu\text{b}$	$150/\text{sec} \times \frac{\Delta k}{k}$
(2) Specific channels			
(a) diffractive $\gamma p \rightarrow \rho^0 p$	yes	$12\mu\text{b}$	$15/\text{sec} \times \frac{\Delta k}{k}$
(b) exchange process $\gamma p \rightarrow \pi^+ n$	yes	20pb at 1000 GeV	$2/\text{day} \times \frac{\Delta k}{k}$ at 1000 GeV
(c) $\gamma p \rightarrow \gamma p$	yes	$0.1\mu\text{b}$	$2/\text{min} \times \frac{\Delta k}{k}$ $-t > 0.15 \text{ GeV}^2$
(3) Inclusive reactions			
$\gamma p \rightarrow \text{hadron} + \text{anything}$	yes	----	large
$\gamma p \rightarrow \gamma + \text{anything}$	yes	$? 5 \text{ nb } (-t > 1 \text{ GeV}^2)$	$20/\text{hr} \times \frac{\Delta k}{k}$
(4) W search	no	$? 10^{-34} - 10^{-37} \text{ cm}^2$	----

IV. PHYSICS WITH ELECTRON-POSITRON COLLIDING BEAM RINGS

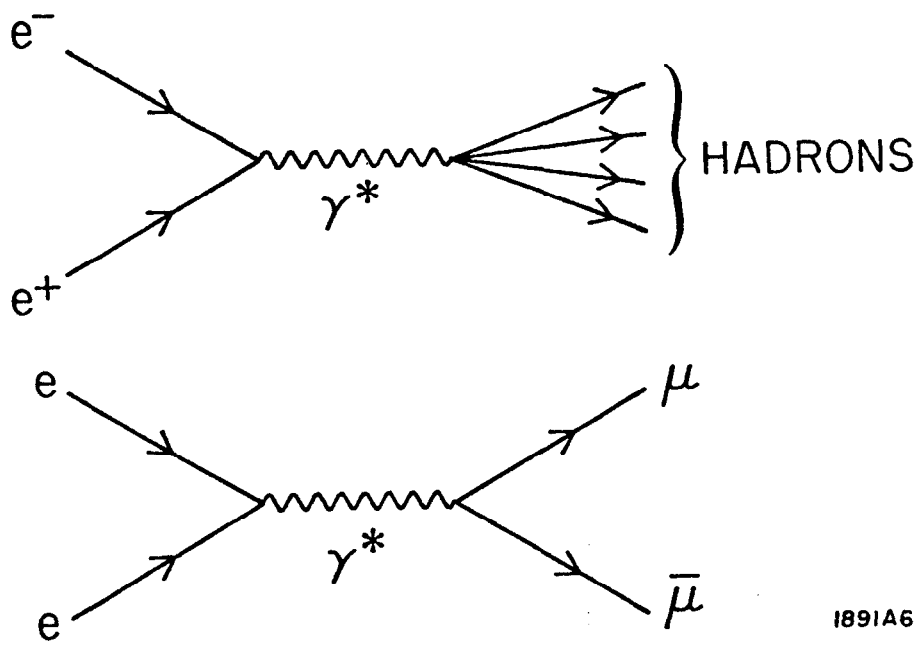
Electron-positron colliding beam rings have opened a beautiful and exciting field that is still in its infancy. When the electron and positron collide, a state of hadrons or a lepton pair with the unique quantum numbers of one unit of angular momentum and odd charge conjugation is produced by an electromagnetic current in the reaction (see Fig. 1):

$$\begin{aligned} e^+ + e^- &\longrightarrow \gamma^* \longrightarrow \text{hadrons} \\ &\longrightarrow e^+ e^- \\ &\longrightarrow \mu^+ \mu^- \end{aligned} \quad (1)$$

The virtual time-like photon γ^* has an invariant (mass)² equal to the square of the total of the collision energy $s = (2E)^2$. The production cross sections, energy dependences, correlations and multiplicities of final particles can all be studied in this one pure channel produced by a single γ . In addition, recent theoretical analyses and experimental evidence suggest that states produced by two photons as illustrated in Fig. 2 can also be studied, as will be discussed later.

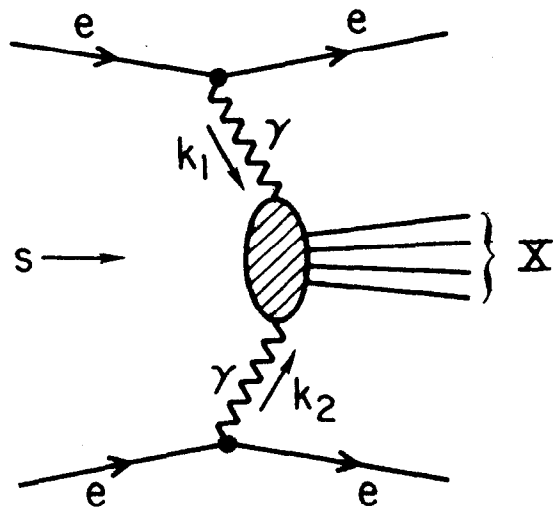
Electron-positron colliding beams in the few-GeV region have been successfully employed for the study of hadronic, leptonic, and photonic final states. In these experiments at Orsay, Novosibirsk and Frascati, vector meson production and decay have been studied; the range of interaction energies over which quantum electrodynamics is known to be valid has been extended to roughly 3 GeV.¹ The first measurements of the total hadronic cross section for colliding electrons to positrons have been made.

With the completion of the CEA bypass colliding beam system and the addition of the SLAC high-luminosity ring, a range of center-of-mass (c.m.) energies can



1891A6

FIG. 1--Electron-positron annihilation into hadrons and muons via the one photon channel.



1922A5

FIG. 2--Final states X produced by two photon annihilation in lepton-lepton collisions.

be covered by the various colliding beam facilities which runs from about 1 GeV to 6 GeV. This c.m. energy range is comparable with that of the existing U.S. proton accelerators which extends up to a maximum of approximately 7 GeV for the Brookhaven AGS, thus allowing for a comparison by energy of the purely hadronic reactions with hadronic final states produced by colliding electron and positron beams.

The addition of a 20-30 GeV colliding beam facility* would allow similar comparisons in the same c.m. energy range as the new generation of proton accelerators (NAL and CERN II). Since this energy for colliding beams is an order of magnitude larger than present energies available, many new features of hadronic and also purely electromagnetic reactions are expected. In the following sections, we specify and discuss some examples of new and important phenomena which would be important to study with the proposed 30-GeV colliding beam facility. From the expected cross sections, we conclude that a luminosity of the order of $10^{32} \text{ cm}^{-2} \text{ sec}^{-1}$ would be appropriate.

A. Behavior of the Total $e^- e^+$ Hadronic Cross Section as a Function of Energy

Experiments in the 1- to 2.5-GeV region have shown² that both the energy dependence and the magnitude of the total hadronic production cross section are roughly the same as those for mu-pair production, i.e., $\sigma_t = \frac{85 \times 10^{-33} \text{ cm}^2}{s} (\text{GeV})^2$. Such large cross sections and point-particle-like energy variations for the hadronic cross section were totally unexpected at the time of the first attempts to build colliding electron and positron beams.³ However, this behavior is what we have learned to anticipate now on the basis of the constituent models of the hadron which have been used successfully in explaining the observed scaling behavior of the deep

*Colliding beam energies given in this section are total energies in the c.m. system unless specifically stated otherwise.

inelastic electron scattering experiments conducted by the SLAC-MIT group.⁴

The important considerations here are to probe experimentally a wide range of variation in s so that we can answer the questions:

- (a) Does the cross section decrease with energy as $1/s$ as for point-like constituents, or does it decrease more rapidly or more slowly?
- (b) Is this dependence asymptotic, i. e., does the energy dependence reach some definite high energy limit? And if it does, what is the nature of the approach to the asymptotic region?

Should the hadronic cross section be comparable to the mu-pair cross section, then we can expect hadronic event rates of order

$$Y = \mathcal{L} \times \frac{2 \times 10^{-32}}{E_{\text{beam}}^2 (\text{GeV})}$$
$$= 0.01 \text{ sec}^{-1}$$

for a luminosity of $10^{32} \text{ cm}^{-2} \text{ sec}^{-1}$ and a beam energy of 15 GeV.

We must, however, be prepared for major surprises in this time-like world of colliding beams in which the electromagnetic current producing hadrons from electron-positron pairs carries very large energy but zero momentum. It is possible that the many resonances that can be produced by this current will lead to even larger than point-like cross-section behavior. For example, if there are particles lying on many linearly rising Regge trajectories, as in Veneziano-type models, or if there are additional vector resonances, they will couple to the electromagnetic current and may lead to very different energy variations of the cross sections. The possible ρ' enhancement at 1.5 ± 0.1 GeV is one such candidate already seen. Another possibility leading to nonpoint-like behavior would be the occurrence of local couplings involving higher spin states. Such contributions

could defer the onset of high-energy limiting behavior, beyond our naive guesses for production amplitudes.

B. Inclusive Production Cross Sections with Detection of One Hadron

With 30-GeV colliding beams, it is possible to study the inclusive reaction

$$e^+ e^- \rightarrow h + \text{anything} \quad (2)$$

for large energy and transverse momentum deposited on the one detected hadron h . In this kinematic region, it may be reasonable to neglect all hadronic masses or constituent masses so that no intrinsic dimensions remain and all cross sections will exhibit a scaling behavior. It is just this scaling behavior that we derive from an elementary point-constituent picture of the nucleon. The energy of the detected hadron can be expressed covariantly by $P \cdot q = E_h \sqrt{s}$, where $w = \frac{2 E_h}{\sqrt{s}}$ defines the fraction of the energy of one of the colliding leptons that appears on the detected hadron in the laboratory frame. In the one-photon approximation (Fig. 1), the scaling law takes the form⁵

$$\frac{d^2 \sigma}{dw d \cos \theta} = \frac{1}{s} \left[f_1(w) + \sin^2 \theta f_2(w) \right] \quad (3)$$

where θ is the angle between the detected hadron and the colliding beam axis. The angular form of Eq. (3) reflects the fact that the electromagnetic current is a vector.

The fundamental questions of crucial importance for this process are:

- (a) Does the inclusive cross section (3) scale with $1/s$?
- (b) What are the magnitudes and w dependences of $f_1(w)$ and $f_2(w)$ for different hadrons such as π , K , N , Σ , Λ , etc? Can they be related in any way to the analogous structure functions for deep inelastic scattering from protons?

(c) How accurate are the predictions of invariance principles at high energies? For example, C invariance of hadronic electromagnetic interactions severely constrains relations between magnitudes and front-back asymmetries when comparing Eq. (2) for h with the hadron being its antiparticle.⁶ As another example, SU_3 symmetry, together with the hypothesis that the electromagnetic current is a U-spin singlet, leads to the following relations between cross sections for the produced hadron h :

$$\begin{aligned}\sigma_{\pi^+} &= \sigma_{K^+} = \sigma_{\pi^-} = \sigma_{K^-} \\ \sigma_{K^0} &= \sigma_{\bar{K}^0} = \frac{1}{2} (3\sigma - \sigma_{\pi^0}) .\end{aligned}\tag{4}$$

It is important to test such relations under kinematic conditions of high energy and momentum transfer. If scaling as in Eq. (3) is verified so that we can neglect the rest masses as well as their differences, equalities such as Eq. (4) should be accurately confirmed.

An important feature of Eq. (2) is that the hadron is being produced with a very large transverse momentum transfer $p_{\perp} = \sqrt{s} \left(\frac{w}{2} \sin \theta \right)$. It is clear that the scaling law, Eq. (3), predicts that a large part of the cross section corresponds to hadron production at large values of p_{\perp} and this is a very important feature of the point-constituent model to test. In contrast, a statistical model⁷ that does not give scaling might lead one to expect exponentially decreasing cross sections with increasing p_{\perp} . Estimates of the production cross section all suggest large cross sections and comfortably observable event rates for processes of the type of Eq. (2) for high-luminosity rings of the type considered here. For example, two different parton, or point-constituent, models analyzed by Berman, Bjorken, and Kogut⁸ suggest for $p_{\perp}^2 \sim 10 \text{ GeV}^2$ event rates of from 1 to 25 events/hr at a total collision energy of 30 GeV and for a luminosity of $10^{32}/\text{cm}^2 \text{ sec}$.

C. Inclusive Production Cross Sections with Detection of Several Hadrons

We can also study the structure of the cross section when many hadrons are observed in an inclusive process

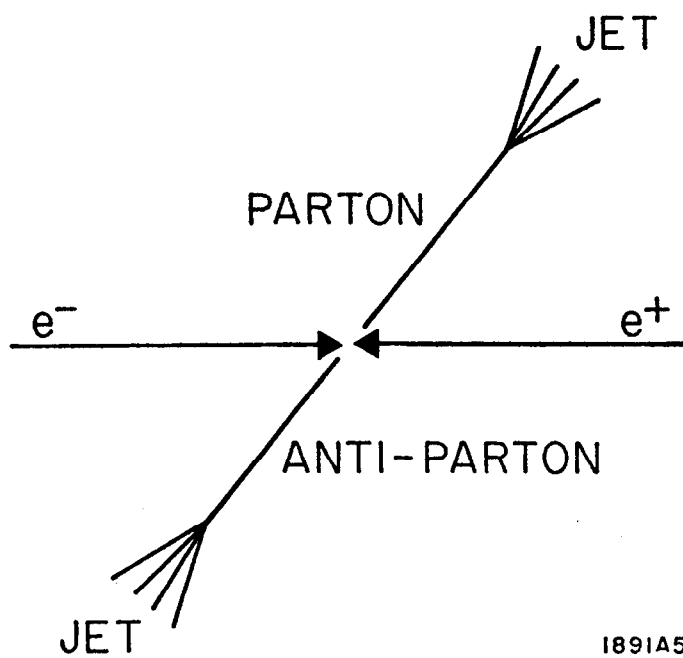
$$e^+ + e^- \rightarrow h_1 + h_2 + \dots + h_n + X. \quad (5)$$

Just as for Eq. (2), we ask how Eq. (5) scales with the colliding-beam energy. In addition, in this case, we can study the hadron multiplicity as a function of energy as well as correlations among the detected hadrons. In a model where the photon decays into a pair of point-like constituents (partons) which subsequently decay into hadrons, we can expect a striking feature: the formation of jets associated with the decay of the constituent partons into the final hadrons. Since the point-like constituents are produced at all angles, these decay jets can appear also at all angles, as illustrated in Fig. 3. That the decaying hadrons should have most of their momentum along the direction of the parent constituent parton is a natural conclusion based on the fact that purely hadronic reactions are dominated by small transverse-momentum processes. Experimental observation, both of jets at large transverse momentum and a scaling behavior, would indeed offer a very striking confirmation of this kind of constituent model.

These examples show that studies of the inclusive processes at high energy and transverse momentum offer the possibility of a wealth of new phenomena which are at present unexplored.

D. Heavy Leptons

Present experiments on two-body (exclusive) hadron production are not sufficiently accurate and do not cover a wide enough range in energy to permit any confident extrapolation to the storage ring energies considered here. On theoretical grounds, however, we would expect hadron form factors falling at least



1891A5

FIG. 3--Electron-positron annihilation into two back-to-back jets.

as fast as $1/s$, which would give unobservably small counting rates for hadron pair production ($e^+e^- \rightarrow \pi^+\pi^-, p\bar{p}$, etc.) at $\sqrt{s} = 30$ GeV with planned luminosities.

However, there may exist point-like heavy leptons in the mass range $3 \leq M_{\mu^*} \leq 15$ GeV which are similar to muons in that they have point-like electromagnetic couplings and no strong interactions. These heavy leptons (μ^*) would be pair-produced just as ordinary muons with cross sections of order the ordinary muon pair cross section. For a mass of the μ^* up to about 13 GeV, the expected counting rate is of order

$$Y = (10^{-34} \text{ cm}^2) \mathcal{L} \approx 10^{-2} \text{ counts/sec} \quad (6)$$

for a luminosity of $10^{32} \text{ cm}^{-2} \text{ sec}^{-1}$.

Since the μ^* would have a very short lifetime ($\tau \approx 10^{-16}$ sec for $M_{\mu^*} \approx 10$ GeV), the detection of these particles would be through their decay products. A high value of the mass would imply many possible decay channels. However, should the purely leptonic modes $\mu^* \rightarrow \mu \nu_\mu \nu^*$ and $\mu^* \rightarrow e \nu_e \nu^*$ have appreciable branching ratios, then the heavy muon pair could be detected by observing an electron-muon coincidence emerging directly from the target point. This type of event is not expected to occur by any direct processes such as $e^-e^+ \rightarrow e^-\mu^+$ or $e^-e^+ \rightarrow \mu^-e^+$, which violate muon conservation. Also, it is expected to occur at only an extremely low rate from the rare leptonic decays of short-lived hyperon-antihyperon pairs, i. e. ,

$$e^+ + e^- \rightarrow \Omega + \bar{\Omega} + \text{anything} \rightarrow (e^- \Xi^0 \nu) + (\mu^+ \Xi^0 \bar{\nu}_\mu) + \text{anything}.$$

A theoretical understanding of the mass spectrum of leptons is one of the most challenging problems in elementary particle physics, and at present it is lacking. All possible experimental investigations relating to this question will be of very great importance.

E. Weak Intermediate Meson (W) Pairs

It has been postulated in analogy to QED that the weak interactions are mediated by massive charge vector mesons. Experimental investigations have been performed using all presently available particle beams and energies with the hope of finding the W. The fact that it has not yet been detected (1971) could mean that its mass is beyond the available energy threshold. If the mass is less than 15 GeV, the 15-GeV storage ring would be an excellent instrument for electromagnetically producing W pairs. This conclusion is based on the assumption that the W-meson has only weak and electromagnetic interactions as is true of the heavy leptons discussed in the preceding section.

The electromagnetic interaction between a photon and a spin-one boson involves, in addition to the charge, the magnetic moment and the electric quadrupole moment of the boson. Electron-positron annihilation may be one of the most effective means of discovering the existence of these vector bosons because of the quite favorable cross section.

The differential cross section in the c. m. system can be written in the form⁹:

$$\frac{d\sigma_{\bar{B}B}}{d\cos\theta} = \frac{1}{32} \frac{\alpha^2}{E^2} \beta^3 \left\{ 2 \left(\frac{E}{m_B} \right)^2 \left| G_1(q^2) + \mu G_2(q^2) + \epsilon G_3(q^2) \right|^2 (1 + \cos^2 \theta) \right. \\ \left. + \sin^2 \theta \left[2 \left| G_1(q^2) + 2 \left(\frac{E}{m_B} \right)^2 \epsilon G_3(q^2) \right|^2 + \left| G_1(q^2) + 2 \left(\frac{E}{m_B} \right)^2 \mu G_2(q^2) \right|^2 \right] \right\} \quad (7)$$

where m_B is the boson mass; E is the c. m. energy; $\beta = p/E$; and G_1 , μG_2 , ϵG_3 are the charge, magnetic moment, and electric quadrupole moment form factors, respectively. They are expected to be roughly constant over the energy region available. If we take $G_1 = 1$, $G_2 = 0$, and $G_3 = 0$, then the total cross section is given by⁷:

$$\sigma_{\bar{B}B} = \frac{2.2 \times 10^{-32} \text{ cm}^2}{m_B^2} \left[1 - \left(\frac{m_B}{E} \right)^2 \right]^{3/2} \left[1 + \frac{3}{4} \left(\frac{m_B}{E} \right)^2 \right], \quad (8)$$

where m_B is in GeV. At high energy, the total cross section becomes constant, whereas the point-like-constituent cross sections discussed earlier decrease with increasing energy as $1/E^2$. Furthermore, taking $\mu G_2 = 1$ rather than zero increases Eq. (8) by a factor $\gtrsim 5$ for $E/m_B \gtrsim 1.2$. Therefore, we expect that electron-positron annihilation into boson pairs would be a very efficient means of producing the particles.

F. Two-Photon Processes

The amplitude for 2-photon annihilation by the process

$$e + e^\pm \rightarrow e + \gamma^* + e^\pm + \gamma^* \rightarrow e + e^\pm + X \quad (9)$$

is illustrated in Fig. 2. Although this process is of order α^4 , whereas the familiar lowest order one-photon contribution is of order α^2 , two factors operate to overcome this added factor of α^2 and to promote the process to importance:

- (1) We expect the cross section for the one-photon process to decrease at high energies as $1/s \sim 1/E^2$ for point-like constituent theories. In contrast, the "almost real" photons radiated by the electrons favor large-impact parameter collisions and the cross section will vary as a constant $1/M_X^2$ where M_X is commonly the threshold mass of the state formed in the photon-photon annihilation.
- (2) We also expect the cross section to be enhanced by familiar logarithmic factors of the form $\ln(E/M_e)$, one for each of the electron

lines, and these are sizable (~ 10 for $E = 15$ BeV). Additional logarithms are also expected, depending on the high-energy behavior of the $\gamma\gamma$ annihilation process.

The significance of this behavior is best seen by looking at Fig. 4 which is taken from the paper of Brodsky¹⁰ et al. and which compares the π -pair production cross section, assuming point pions in the one- and two-photon processes

$$e^+ + e^- \rightarrow \gamma^* \rightarrow \pi^+ \pi^-$$

$$e^+ + e^- \rightarrow e^+ + e^- + \gamma + \gamma \rightarrow e^+ + e^- + \pi^+ + \pi^-$$

Evidently the two-photon cross section is very important. Of course, pions are not point charges and there are structure corrections. An estimate of these structure effects in terms of a σ resonance is shown in Fig. 4. They further increase the 2γ contribution. In particular, the region near the production threshold for $\gamma\gamma \rightarrow 2\pi$ is important.

We see here, then, the possibility of studying the entirely new field of hadronic states with even C as produced from two photons. The cross sections are large. By detecting the final leptons and determining the energies k_1 and k_2 of the two colliding photons, one can measure in detail the differential cross section for two colliding "almost real photons" to produce any observable final state.

From two-body final states this process can also be generalized to multi-body hadronic states. For example, the production of hadrons of high transverse momentum in the inclusive process

$$e^+ + e^- \rightarrow \gamma + \gamma \rightarrow h + X + e^+ + e^-$$

would, in principle, be measurable; h denotes a hadron detected along with the lepton pair and X denotes all other hadrons that are not detected. Parton-antiparton-pair production $\gamma + \gamma \rightarrow q + \bar{q}$ provides a mechanism for producing hadrons

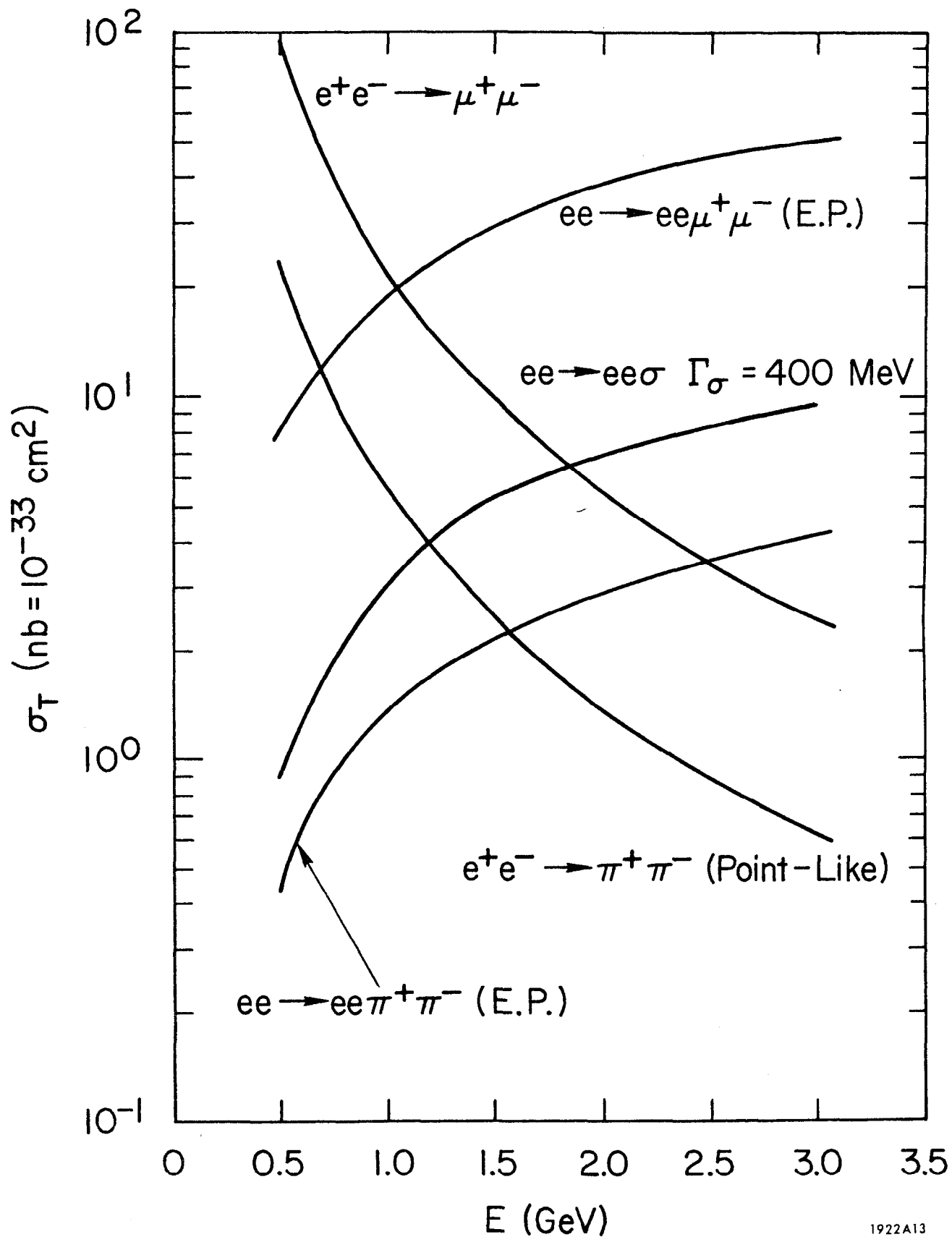


FIG. 4--The rising two photon annihilation cross sections as a function of total c.m. energy plotted along with the falling one photon annihilation channel.

of high transverse momentum in a manner similar to that of the one-photon annihilation channel described in the preceding section. Calculations of such cross sections indicate they are large for low transverse momenta of the detected hadron and they fall off for large values. Measurement of this decrease will provide further important information on the constituent structure of hadrons. In the parton model of Ref. 8, the counting rates are expected to be at least 10^{-3} times smaller than for the process of Eq. (2) for transverse momenta $p_{\perp} > 2$ GeV. Although this counting rate may be very small, it will be important to probe to as large a value of p_{\perp} as can be observed.

The two-photon process also provides a way for probing the structure of the photon by deep inelastic scattering of electrons from photons.¹¹ In this case, the deep inelastic scattering of electron e to e' takes place from the virtual, almost real, photon spectrum of the "target electron":

$$e + \gamma (\text{real}) \rightarrow e' + \text{anything} .$$

The projectile electron is kinematically constrained to deliver large q^2 and ν as in the SLAC experiments on deep inelastic electron scattering from photons. The recoil of the target electron with known momentum and at small angle is also detected so that the almost real target photon has a known frequency and the conditions for Bjorken scaling are satisfied. This process can be measured with high-luminosity storage rings and if scaling is verified, it will provide a direct measurement of the photon's parton structure. Estimates of the process using a parton model⁷ indicate that the counting rate will be comparable to the case of the hadronic inclusive reaction with rates of the order 1 to 25 events per hour for a luminosity of $10^{32}/\text{cm}^2 \text{ sec}$.

Existing colliding-beam storage rings at Orsay, Novosibirsk, and Frascati have measured these processes at energies and momentum transfers of several

GeV and have verified that QED is valid in that region.¹ One way of representing these experimental results is by expressing the smallest possible value of a cutoff has to be larger than 2 - 3 GeV. By increasing the value of the collision energy of the incident pair from 6 GeV to 30 GeV, the large ring will allow precision tests to probe for possible modifications resulting from cutoffs in the 100 - 200 GeV region. The validity of electrodynamics has now been established over 24 orders of magnitude from several earth radii down to less than a nucleon Compton wavelength. These experiments would extend our knowledge yet another order of magnitude by probing distances as small as 10^{-16} cm.

References

1. V. L. Telegdi, Invited paper to The Amsterdam International Conference on Elementary Particles (North-Holland, Amsterdam) June 30 - July 6, 1971.
J. J. Sakurai, Balaton Symposium on Hadron Spectroscopy, ACTA Fysica, Keszthely, Hungary, September 7 - 11, 1970.
2. See S. D. Drell, Rapporteur Report to The Amsterdam International Conference on Elementary Particles, June 30 - July 6, 1971.
3. SLAC Staff, 1966 SLAC Storage Ring Proposal, September 1966.
4. For general review, see F. Gilman, Proceedings of the Fourth International Conference on Electron and Photon Interaction at High Energy, Daresbury Nuclear Physics Laboratory, Liverpool, England, September 1969.
5. S. D. Drell, D. Levy and T. M. Yan, Phys. Rev. D1, 1117 (1970).
6. For tests of invariance principles which are not restricted to the one-photon approximation, see A. Pais and S. B. Treiman, Phys. Rev. 187, 2076 (1969).
7. J. D. Bjorken and S. J. Brodsky, Phys. Rev. D1, No. 5, 1416 (1969).
8. S. M. Berman, J. D. Bjorken and J. B. Kogut, SLAC Report No. 944 (1971).
9. N. Cabibbo and R. Gatto, Phys. Rev. 124, 1377 (1961).
10. S. J. Brodsky, T. Kinoshita, H. Terazawa, Phys. Rev. Letters 25, 972 (1970).
11. S. J. Brodsky, T. Kinoshita, H. Terazawa, Cornell Preprint (1971);
T. Walsh, DESY Preprint 71-15 (1971).